THE PROLIFERATIVE RESPONSE OF HEPATIC PEROXISOMES OF NEONATAL RATS TO TREATMENT WITH SU-13 437 (NAFENOPIN)

W. STÄUBLI, W. SCHWEIZER, J. SUTER, and E. R. WEIBEL

From the Research Department of the Pharmaceuticals Division of CIBA-GEIGY Limited, CH-4002 Basel, Switzerland, and the Department of Anatomy, University of Berne, CH-3012 Berne, Switzerland

ABSTRACT

The repeated administration of the hypolipidemic agent Su-13 437 (nafenopin) to neonatal rats roughly doubled the number of peroxisomes in the liver tissue and caused a sixfold volumetric expansion of the peroxisomal compartment. During the proliferative response, the size-distribution of the peroxisomes was reversibly altered, enlarged particles appearing in numbers varying according to the dose given. By means of a new method for quantitative autoradiography, it was shown that (*a*) the concentration of silver grains over peroxisomes was comparable to that found over the endoplasmic reticulum; (*b*) the peak incorporation of [^{3}H]arginine into the peroxisomes was delayed in comparison with that into the endoplasmic reticulum; (*c*) the label, once incorporated into the expanding peroxisomal compartment, displayed the same shift to large particles as did the whole population. These results are compatible with the biosynthetic pathway for peroxisomal catalase proposed earlier (cf. reference 12), and with the notion that the drug-induced size-shift might have resulted from progressive growth of a particular class of peroxisomes formed in the presence of the agent. Evidence is presented to show that during the recovery period the larger peroxisomes are removed preferentially.

In a series of reports, we have shown that two hypolipidemic drugs of the α-aryloxyisobutyric acid type, clofibrate (CPIB)[1] and CIBA Su-13 437, are endowed with the capacity to elicit the induced state and to expand the peroxisomal compartment of male rat liver parenchymal cells (24–26, 69). These observations were subsequently confirmed and extended by several research groups (reviewed in references 2, 30, 56, 70). The biosynthesis and precise metabolic function(s) of peroxisomes (microbodies) in normal or in experimentally altered mammalian cells are still not fully understood (12, 13, 56, 70), although in the past few years considerable progress has been achieved with regard to the biosynthesis of peroxisomal constituents (37, 38, 62). In addition, interest in the biology of peroxisomes has been rekindled by a large number of morphological observations leading to the concept of the ubiquitous distribu-

[1] *Abbreviations used in this paper:* CPIB, clofibrate, Atromid S; DAB, diaminobenzidine; ER, endoplasmic reticulum; PO, peroxisome(s) (microbody); RER, rough-surfaced endoplasmic reticulum, SER, smooth-surfaced endoplasmic reticulum; Su-13 437, CIBA Su-13 437 (nafenopin).

tion of these organelles among mammalian cells (31).

Inasmuch as the peroxisomes constitute a minor organelle in the rat hepatocyte (44, 78), the proliferating effect of compounds of the α-aryloxyisobutyric acid type on these structures might be utilized to investigate, *in situ*, some aspects of their biosynthesis in quantitative terms. In this report, the proliferative response of these organelles in the hepatocytes of immature rats treated repeatedly with Su-13 437 will be described in the light of a morphometric, autoradiographic, and dimensional analysis.

MATERIALS AND METHODS

Animals

Newborn albino rats (Wistar-derived) were used. The pregnant dams were fed standardized laboratory chow (Nafag no. 890) ad lib.

Treatment with Su-13 437

Six newborn rats of similar weight were taken from each litter and divided into two groups of three. Su-13 437 suspended in 2% carboxymethylcellulose (CMC) was administered by intubation to the rats of the experimental groups in daily doses of 100 mg/kg body weight. The first dose was given on the 5th day postpartum, and the treatment continued for five consecutive days. The animals thus received the last dose of Su-13 437 at the age of 9 days (cf. Fig. 1). The other three animals from the same litter were treated in the same manner with CMC and served as controls.

Experimental Time Schedule

As exemplified in Fig. 1, the observation period was divided into two parts. During the first part (progression), five consecutive doses of Su-13 437 were administered to induce a high proliferation rate of peroxisomes (PO). The drug treatment was then discontinued. During a subsequent 8-day recovery period, the disposal of excess PO was studied. The labeled amino acid was injected simultaneously with the third dose of the drug, and this point was designated as "zero" time (cf. arrowhead on the abscissa of Fig. 10). For the selection of labeling intervals, some additional aspects of the biosynthesis of PO were considered. It has been shown that the specific activity of an important peroxisomal enzyme, catalase, reached a peak in the rough-surfaced endoplasmic reticulum (RER) 20–30 min after the injection of a radioactive amino acid (27). The selection of 20 min after the administration of the isotope as the first determination time made allowance for this biochemical finding. By injection of a reusable radioactive amino acid, the half-life of hepatic PO has been estimated to be 3–4 days (55). Therefore, we chose the 3rd day after administration as a further determination time; within the interval between the two selected times, further determinations were made at 6 h and 1.5 days. In addition, the tissue was analyzed 6 and 10 days after the injection of the label. As detailed in Fig. 1, the first three intervals (20 min, 6 h, and 1.5 days) fall within the progression phase, and the last three (3, 6, and 10 days) within the recovery period. At the end of the experiment (10 days), the animals were 17 days old. At the times stated, the rats were lightly anesthetized with ether and sacrificed by decapitation.

Injection of the Isotope

Generally labeled DL-[^{3}H]arginine monochloride (Radiochemical Centre, Amersham, England; specific activity 1,200 mCi/mmol) was injected into the saphenous vein of three rats per determination time-point. Each rat received 2 mCi in 0.1 ml of distilled water. The site of injection was covered with a collodion film. Because drug-treated animals did not tolerate ether inhalation, they were anesthetized with a mixture of 95% CO_2 and 5% O_2 given through a mask.

Preparation of the Tissue

Although it has been claimed that formaldehyde is a more reliable fixative for autoradiographic purposes than osmium tetroxide (8, 52), the latter was chosen to permit comparison with earlier morphometric data published by our and other laboratories. The liver tissue was fixed for 2 h in cold phosphate-buffered OsO_4, dehydrated in acetone, and embedded in Araldite (Ciba-Geigy, Basel, Switzerland). The procedures adopted in preparing and staining thin sections are described below. It should be mentioned that the morphometric and the autoradiographic analyses were performed on the same animals.

Autoradiographic Procedures

The bubble method described by Caro (10) was used and in our hands afforded reasonable reproducibility of grain monolayers. Thin sections (silver to gold, corresponding to about 850 Å on the thickness scale of Salpeter and Bachmann (65) were prepared on a LKB-4800 ultrotome (equipped with a diamond knife), transferred to 200-mesh grids covered with a collodion-carbon film, and stained with aqueous uranyl acetate (10 min at 60°C). The grids were then attached to Parafilm ribbons adhering to a glass slide and covered with Ilford L4 emulsion. Bubbling of the emulsion was performed with "Cyklon," an aquarium-type pump (J. Demuth, Wallisellen, Switzerland). The coated grids were packed into Clay Adams boxes (Clay Adams, Inc., Div. of Becton, Dickinson, Co., Parsippany, N.J.) in the presence of silica gel. Finally, the boxes were placed in exsiccators containing silica gel and stored at 4°C. During exposure, the desiccating material was replaced every 3 wk. Each box contained (*a*) experimental grids that served for the quantitative analysis of autoradiographs; (*b*) grids used

to determine the optimal exposure time; (*c*) grids covered with nonradioactive sections for the assessment of the background fog; (*d*) grids without sections for monitoring the time-course of the background fog development. The optimal exposure time was considered to be attained when the ratio of silver grains on grids covered with labeled sections (*b*) to silver grains on grids without sections (*d*) was maximal. This point was reached after 5 mo exposure.

The exposed preparations were developed for 5 min with Kodak D-19 developer at 20°C. Finally, the autoradiographs were stained for 10 min with lead acetate (63). At the end of the exposure time, the average background was 2 grains/1,000 μm^2 (range: 1–5 grains/1,000 μm^2) and could accordingly be disregarded.

Quantitative Evaluation of Autoradiographs

Only autoradiographs obtained from animals treated with Su-13 437 were analyzed. The quantitative procedure was based on the "95% probability" circle method of Whur et al. (79).[2] A circle (resolution-boundary circle) 12.4 mm in diameter (corresponding to magnification level I of the morphometric procedure) was engraved on a transparent plexiglass disk about 7 cm in diameter (cf. *inset* of Fig. 9). On the perimeter of this circle, five equidistant points were marked. The autoradiographs were then analyzed as follows: The negatives (×2,500) were transformed to positives by contact printing. These were projected onto a screen by means of a table projector unit (final magnification ×27,500). The transparent disk was randomly superimposed on the projector image of the autoradiograph in such a way that the engraved resolution-boundary circle enclosed a silver grain. The probability that one or another of the underlying subcellular compartments (e.g., endoplasmic reticulum [ER], mitochondria, PO, etc.) might, through the spread of radiation, have contributed radiant energy to the developed silver grain was then estimated with the aid of the five marks engraved on the circumference of the probability circle. If, for example, two of the marks "hit" the RER compartment and the other three a PO, the chance that the RER and/or the peroxisomal profile might have been the source of radiation that generated this particular silver grain was estimated to be 2 in 5 or 3 in 5, as the case may be (cf. *inset* of Fig. 9). A subcellular compartment comprising the whole probability circle was therefore rated as 5/5. The calculations for estimating the label distribution will be given below. The autoradiographic analysis was based on about 24,000 silver grains. When the labeling was most dense (6 h), the average grain density of the autoradiographs was estimated to be 42/82 μm^2 (cf. Fig. 8), as compared to 8 grains in the case of lowest grain density (10 days).

[2] For criticism of the "95% probability" circle concept, consult Salpeter and McHenry (66).

Morphometry

GENERAL COMMENTS: The preparations subjected to morphometric analysis were identical to those used for autoradiographic assessments. The specimens were collected essentially according to Weibel et al. (78). Three rats treated with Su-13 437 and three controls given CMC only were examined at each of the appointed times. Altogether, 36 rats were used.

PRIMARY SAMPLE: This consisted of about 20 tissue blocks (~1 mm^3) collected from three different regions of the liver.

SECONDARY SAMPLE: From the pool of tissue blocks, five were randomly selected per animal (i.e., a total of 30 blocks were examined on each occasion). Thin sections were cut from each block (average thickness ~850 Å). One section of good quality was chosen for the morphometric analysis. Accordingly, altogether 15 thin sections per group (three animals) were available for examination each time.

TERTIARY SAMPLE: From each thin section, six random electron micrographs were made on a Siemens Elmiskop Ia at two magnification levels: × 2,500 for level I and × 6,000 for level II. The total of 90 micrographs per group (three animals) and time interval were analyzed. The selected tissue areas were photographed on 35-mm film strips, which were contact-printed on film. These positive prints were examined by means of a table projector unit yielding an 11-fold secondary magnification. The final magnifications were thus × 27,500 for level I and × 66,000 for level II. The magnification was calibrated with the help of a carbon grating replica (Ernest F. Fullam, Inc., Schenectady, N.Y.) having 28,800 lines/in.

CHOICE OF TEST LATTICES: For point-counting at level I, a rectangular frame (192 × 288 mm) containing a double-lattice grid (891 test points, ratio 1:9) was used. The level II micrographs were analyzed by means of a square frame (240 × 240 mm) which comprised a multipurpose test screen (21 test lines, 84 mm of length).

DESCRIPTION OF CELL COMPARTMENTS: At the magnification level I, point-counting (to determine the specific volume of different compartments) and profile-counting (to determine the specific number of mitochondria, peribiliary dense bodies, lipid droplets, and peroxisomes) were performed. The following cell compartments were considered: extrahepatocytic space, nucleus, mitochondria, peroxisomes (microbodies), peribiliar dense bodies (including cytolysomes or autophagic vacuoles), lipid droplets, RER (including intercisternal and pericisternal areas containing apparently "free" ribosomes or polyribosomes), and SER (including Golgi membranes and glycogen areas). It should be noted that the present *en bloc* definition of the RER was adapted for autoradiographic purposes and presupposes that this organelle is composed of an intracisternal lumen bounded by cisternal membranes with attached ribosomes and the intercisternal and pericisternal ground substance, in which generally no structures other than

ribosomes are included.

LEVEL II: This higher magnification level allowed a more refined point-counting and included RER, SER, Golgi apparatus (comprising stacked lamellae and organelle-associated secretory vesicles containing very low density lipoprotein particles), compact areas of apparently "free" ribosomes or polyribosomes, and the cytoplasmic ground substance (comprising the interparticulate space not already assigned, according to the above definitions, to other compartments).

Although all the compartments listed above were considered in the morphometric analysis, only those conceivably related to the biosynthesis of PO will be dealt with in this report.

RECORDING OF DATA AND COMPUTATIONS: The primary counts were processed according to criteria already discussed (78) by means of a morphometric computer program (19). The results were related to a liver volume corresponding to 100 g of body weight of the animal and thus represent specific dimensions (cf. reference 78). Previous considerations regarding possible sources of error in the morphometric analysis of tissues (78) also apply to the present work.

DETERMINATION OF SPECIFIC WEIGHT OF LIVERS: In order to relate the morphometric parameters to the liver volume, determinations were made of the average specific weight of 10 livers each from 10-day-old rats treated with either Su-13 437 (mean specific weight: 1.0594 $g \cdot ccm^{-1}$) or CMC (mean specific weight: 1.0632 $g \cdot ccm^{-1}$). There was no statistically significant difference between the two means.

ADDITIONAL RECORDINGS: At magnification level I, the diameters of peroxisomal profiles were recorded on a Zeiss Particle Size Analyzer (Carl Zeiss, Oberkochen, Germany). The values obtained were then computed into peroxisomal diameters by applying the Wicksell transformation (4, 80). From level II micrographs, the ratio of peroxisomal profiles containing a nucleoid (or core) to those lacking such a structure was estimated in thin sections of the livers of control and treated animals. For each group and each experimental time-point, 102–293 profiles were recorded. To obtain a numerical estimate of the portion of the whole population of peroxisomes made up by the so-called (anucleoid) microperoxisomes (cf. reference 49), we took into consideration a statistical relationship between the size of the nucleoid and that of the whole PO, i.e., that the chance of a nucleoid-containing PO revealing the presence of a nucleoid within a given profile is proportional to the ratio of the nucleoid diameter to the particle diameter. For example, a ratio of 0.43 would mean that in a population consisting exclusively of nucleoid-containing PO, ~43% of the profiles would have revealed the presence of a nucleoid (cf. Table I). This ratio was determined for 100 randomly selected PO each in sections prepared from livers of control and treated (1.5 days) rats.

Correlation between Autoradiographic and Morphometric Data

It has already been mentioned that the counting of developed silver grains, their assignment to the different subcellular compartments, and the morphometric recording were performed on the same micrographs. To begin with, the grain counts of the individual compartments were expressed per hepatocytic unit volume, i.e., number of grains on compartment/cm^3 of hepatocyte. This mode of expression, the radiation label density, indicates the relative labeling intensity of the different compartments, disregarding their actual contribution to the cell volume. A second characteristic, the specific radiation label density, was then calculated. It reflects the grain counts per unit volume of a given compartment, i.e., number of grains on compartment/cm^3 of compartment. The rationale of this procedure is as follows: to estimate the relative volume of the compartments (i.e., volume density V_v) a lattice of random points was spread over the sections, and the points falling on compartment i, P_i, were recorded, yielding the volume density of i in the cell being $V_{Vi} = P_i/P_c$, where P_c denotes the number of points falling on the hepatocytes. To estimate the probable distribution of the label radiation source, a second lattice of points was used; however, these were "grain-associated" rather than random, i.e., they were represented by the five points on the circumference of the 95% probability circle that was fitted around the grain (cf. Fig. 9). The number of these points falling onto a profile of compartment i, G_i, was also recorded. It can be postulated that this second point count is biased by any preferential location of the label in one or another of the compartments. The bias due to the relative label density in compartment i can be obtained, as an initial approximation, from the ratio G_i/P_i, i.e., the ratio of grain-associated to random point hits on i.

To calculate the "true" label density in the cell or compartment volume, the section thickness T had to be considered. Likewise, the profile area of the cell, A_c, over which grains were counted, or of the profile compartment i, A_i, had to be expressed in absolute terms; because we used a square point lattice of point spacing d, these areas were obtained by $A_c = P_c \cdot d^2$ and $A_i = P_i \cdot d^2$, respectively. *The radiation label density* in the cell was hence

$$R_{Vi}^{\cdot} = G_i/5 \cdot A_c \cdot T = G_i/P_c\,(5 \cdot d^2 \cdot T),$$

where the coefficient 5 is related to the fact that five points were counted for each grain. *The specific label density* in compartment i is accordingly

$$R_{Vi}^{+} = G_i/P_i\,(5 \cdot d^2 \cdot T).$$

Hence, it is readily apparent that the formula for the specific label density corresponds to

$$R_{Vi}^{+} = R_{Vi}^{\cdot}/V_{Vi}^{\cdot},$$

the ratio of radiation label density to volume density for compartment i in the hepatocytes.

Millipore Filtration

Small aliquots (~0.3 ml) of the resuspended (0.25 M sucrose) mitochondria-rich MLP fraction were fixed for 30 min at 4°C in a 4% formaldehyde-1.25% glutaraldehyde mixture and filtered through Millipore filters (pore size: 0.1 μm) according to the procedure outlined by Baudhuin et al. (6). The pellicles obtained were washed with cacodylate buffer (~2 ml) and their surfaces stabilized by the addition of a few drops of liquid agar. The filters with adhering pellicles were removed from the filtration unit and processed by means of the diaminobenzidine (Fluka, Buchs, Switzerland) reaction (7) to demonstrate peroxidase activity; control preparations were incubated in a medium lacking hydrogen peroxidase, or containing 0.01 M 3-amino-1,2,4-triazole (Fluka, Buchs, Switzerland).

Biochemistry

ANIMALS: Biochemical estimations were performed in five to six animals per experimental or control group. The treatment schedule already described was carefully duplicated, except that no analysis was made 20 min after the third dose of Su-13 437.

TISSUE FRACTIONATION: The weighed livers were homogenized in 0.25 M sucrose with the aid of a glass-teflon homogenizer to obtain a 5% homogenate. The homogenate was centrifuged at 8,500 g for 30 min (MSE Mistral 6 L), and the resultant pellet was carefully rehomogenized in 0.25 M sucrose. Debris and nuclei were separated by centrifugation (600 × g for 20 min), and the supernate was spun at 8,500 g for 30 min. The resultant pellet was washed once under identical conditions. This fraction was composed of elements of the ER, mitochondria, lysosomes, and peroxisomes, and is accordingly designated the MLP fraction. The 8,500 g supernate was centrifuged at 105,000 g for 60 min (Spinco L2-65B, rotor 60 Ti), yielding a microsomal pellet and a supernate (fraction S) containing the soluble components of the cytoplasm.

ENZYME ASSAYS: The activity of catalase was estimated in the MLP ("particulate" activity) and the S ("free" activity) fraction, 15 min after the addition of 1% (vol/vol) Triton X-100 (5). The enzyme assay followed a procedure described by Creasey (11). The activity of the peroxisomal core enzyme urate oxidase was determined according to de Duve et al. (14).

PROTEIN DETERMINATION: The protein content of the fractions was estimated by the procedure of Lowry et al. (45).

RESULTS

Proliferative Response of Peroxisomes

DIMENSIONAL ASPECTS: In control animals the specific volume of PO remained relatively constant throughout the duration of the experiment at a level comparable to that determined in adult rats (Fig. 1). The same holds good for other peroxisomal parameters such as the mean volume (Fig. 2), the specific number (Fig. 3), the frequency of nucleoid-containing profiles (Fig. 4), and the size distribution (Figs. 5 and 6). Tsukada et al. (74) have reported that during a comparable postnatal interval several peroxisomal characteristics did not change; however, in contrast to our findings, they observed a reduction of the particle size.

The distribution of true diameters of PO, as determined by the Wicksell transformation of measured particle diameters (4, 80), is shown by the stippled histograms in Fig. 5. It can be seen that the diameters are distributed around the median values which are clustered within a fairly narrow interval, i.e., between 0.39 and 0.43 μm. Although these diameter distributions were based on comparably large numbers of particles (~1,000 per experimental time-point), their contours were rather "notched." In fact, statistical comparison by means of the χ^2 test of the individual distributions in the three animals examined per time interval showed that the PO of these three animals could not be regarded as belonging to the same sample. The reason for this finding could be either that the number of measured particles per animal was too small to fill all the size classes evenly, or that the population representing the control animals was itself composed of different particle types, which entered the analysis with a variable probability. In fact, recent reports have furnished evidence that rat hepatocytes (and other cell types) may contain at least two different kinds of PO: the so-called microperoxisomes (diameter ~0.20 μm) and the commonly described mature variety (49). In addition to microperoxisomes, peroxisome-like "Q" particles (diameter ~0.25 μm) have recently been reported to occur in rat hepatocytes (77). Although the morphogenetic and biogenetic relationships between these two sets of structures remain to be elucidated, both kinds apparently lack a matrical core. In the context of the present experiments, it is important to have a notion of the numerical contribution of the microperoxisomes to the whole peroxisomal population. These particles merit particular interest because it may be assumed that in rat liver they could represent the progenitors of the mature core-con-

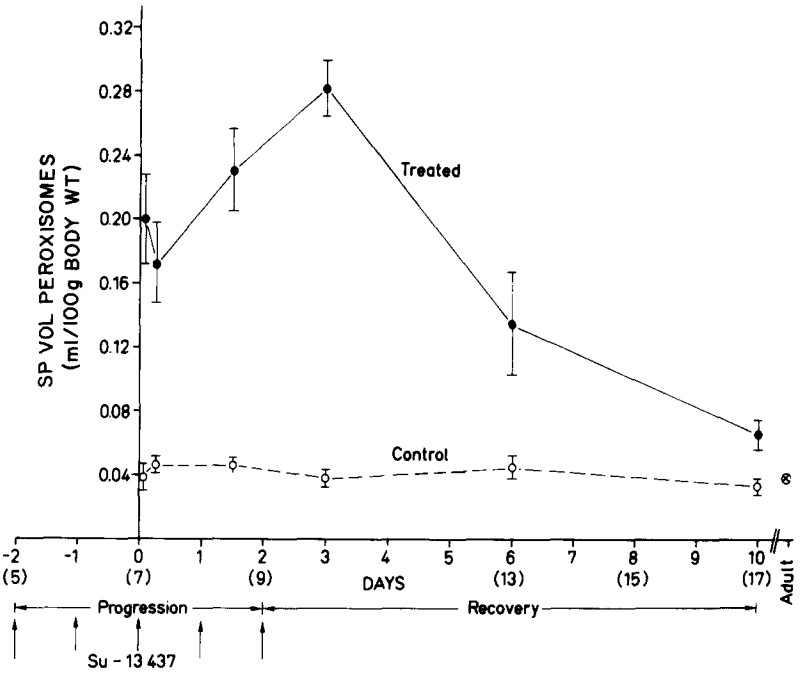

FIGURE 1 Specific volume of peroxisomes. Treatment of the animals with Su-13 437 started on the 5th postnatal day (denoted by −2 on the abscissa). The rats received five consecutive doses of the drug (arrows), the last being given on the 9th day postpartum (day 2). The radioactive precursor was administered together with the third dose of the drug on the 7th postnatal day which was designated time zero (cf. Fig. 10). Accordingly, the whole experiment was divided into two periods. During the first interval (which included the sampling times: 20 min, 6 h, and 1.5 days), the animal received the drug until day 2 (progression). Medication was then stopped, and the animals were observed during a period of 8 days (recovery); this second period included the times: 3, 6, and 10 days. The duration of the experiment thus covered a postnatal period extending from 7 (day 0) to 17 days (day 10). The level of significance of treated animals, as compared with controls, was $P < 0.001$ throughout. Standard errors are indicated. The value for the untreated adult rat was taken from reference 78.

taining PO (50) and thus play a decisive role in the proliferative response of PO to treatment with Su-13 437. According to the statistical considerations outlined in Materials and Methods, the ratio of nucleoid to particle diameter was determined for 100 PO from control sections and found to be 0.57. Therefore, it could be expected that if the counting of nucleoid-containing PO had been performed on a particle sample composed exclusively of nucleoid-containing PO, ~57% of the profiles would have been rated as anucleoid (Table I). As can be seen in Fig. 4, the proportion of anucleoid peroxisomal profiles in control animals was found to vary (insignificantly) between 61 and 76% (mean: 70%) of the total particle population (Table I). Upon comparison of the results (Table I) obtained from the determination of the nucleoid-to-particle size ratio (57% of anucleoid particles) and the counting of core-less PO profiles (70%), it would appear that our counts of anucleoid profiles included only ~13% of truly (anucleoid) microperoxisomes and/or "Q" particles. Similar determinations performed on PO from treated (1.5 days) animals revealed that in spite of the expansion of the PO compartment, the proportion of microperoxisomes remained virtually unchanged (Table I). From these observations, it is concluded that the so-called microperoxisomes make up a minor fraction of the total PO volume; this part of the PO population is not altered to any significant extent during drug-induced PO proliferation, thus most probably excluding a precursor-product relationship between microperoxisomes and mature PO. As represented in Fig. 4, the proportion of anucleoid PO profiles increases considerably during drug treatment. By determining

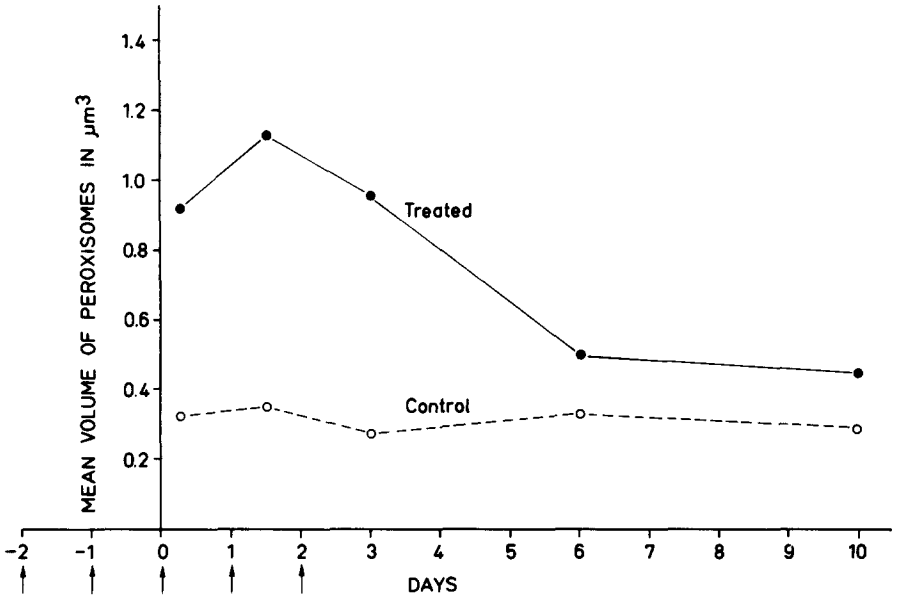

FIGURE 2 Mean volume of peroxisomes. The values are derived from a Wicksell transformation of profile diameters measured by means of a particle size analyzer. Note that this parameter attained its peak value earlier (i.e., on day 1.5) than its specific volume (cf. Fig. 1).

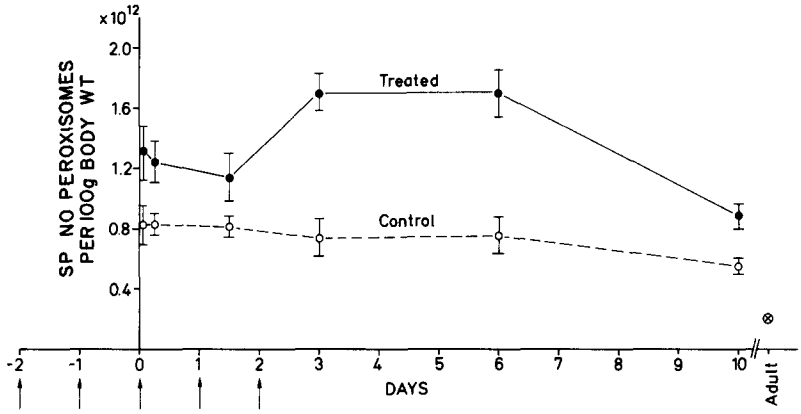

FIGURE 3 Specific number of peroxisomes. In control animals the value of day 10 is significantly lower ($P < 0.01$) as compared with 20 min. The level of significance of treated rats, as compared with controls, was $P < 0.001$ throughout. For treated rats, the values attained on days 3 and 6 were significantly higher ($P < 0.001$) in comparison with 1.5 days. Similarly, the value of day 10 was significantly lower ($P < 0.001$) than that determined at the beginning of the experiment (20 min). Standard errors are indicated. The value for the untreated adult animal was taken from reference 78.

the apparent diameter of the nucleoids in 100 randomly selected PO profiles in each of the control and treated groups, it was shown that the mean apparent diameter of the nucleoid (~0.18 μm) was not significantly changed as a result of the administration of the drug. Therefore, the increase in the frequency of anucleoid particles (Fig. 4) was not due to a reduction in the size of the core material attributable to the influence of Su-13 437. Consequently, the ratio of the nucleoid diameter to the particle diameter suffered a roughly twofold decrease (from 0.43 to 0.27) in the presence of the drug.

Treatment of 5-day-old rats with Su-13 437

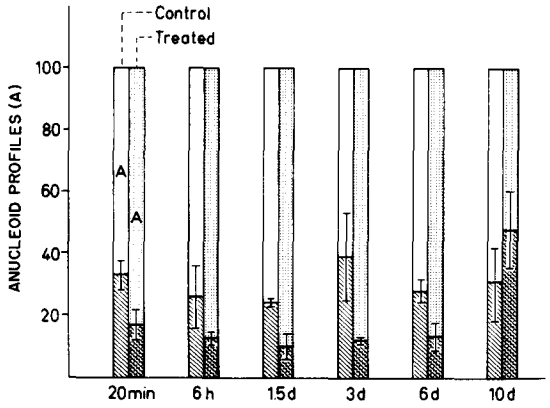

FIGURE 4 Frequency of anucleoid (core-less) peroxisomal profiles in percent of total peroxisomal profiles. The upper parts of the columns marked *A* represent the anucleoid portion of the total peroxisomal profiles. The data are based on 725 and 1,476 profiles for control and treated animals, respectively. Standard errors are indicated.

caused a marked expansion of the peroxisomal compartment. There was a dose-related increase in the specific volume of PO in the hepatocytic cytoplasm, which reached its maximum on the 3rd day, i.e., one day after the administration of the last dose (Fig. 1). Similarly, the mean volume of PO was increased, with a peak on day 1.5 (Fig. 2). The number of PO was also augmented and reached a plateau between day 3 and day 6 (Fig. 3). The distribution of PO diameters as obtained from the Wicksell transformation clearly showed that the administration of Su-13 437 to neonatal rats caused an increase in the particle diameters, resulting in a considerable shift in the distribution toward higher values (Fig. 5). After treatment with four doses, the mean particle diameter increased from ~0.4 to ~0.6 μm. Consequently, the average PO of treated animals was enlarged by a factor of ~3.5 (Fig. 2). From the distribution of diameters represented in Fig. 5, it can be seen that during the drug-induced expansion of the peroxisomal compartment, e.g., at 6 h and 1.5 days, fewer of the smaller particles falling within the distribution characteristic of the control animals were present in the treated rats. This numerical deficit in particle sizes belonging to the control distribution is clearly evident if an attempt is made to evaluate it graphically. In Fig. 6, the drug-induced distribution of peroxisomal profile diameters is represented. If it is assumed that this distribution is a composite one comprising particles of control and drug-induced sizes, the proportion of the latter can be estimated by subtracting, in each diameter class, the control value from the counts obtained from treated animals. The resultant histograms (Fig. 6) might thus reflect the size variations of PO due to the drug treatment. From Fig. 6, the following conclusions may be drawn: the

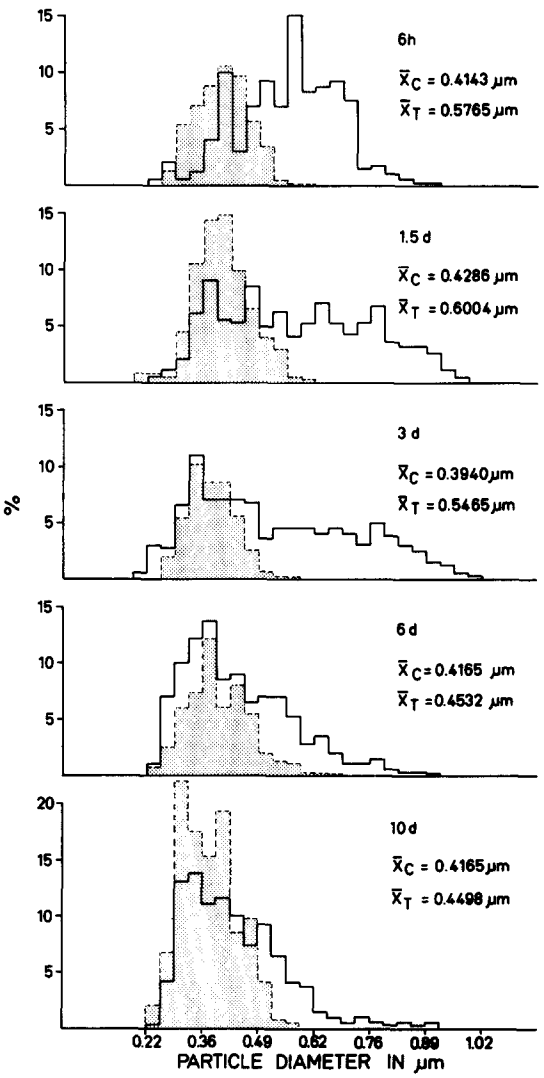

FIGURE 5 Distribution of true peroxisomal diameters as obtained by Wicksell transformation. The values refer to identical tissue areas used for determination of profile diameters. The stippled areas represent the distribution of peroxisomes in the controls, whereas the solid lines indicate the distribution pattern in treated rats. The mean diameters of peroxisomes of control and treated animals were denoted by $\bar{X}_C$ and $\bar{X}_T$, respectively.

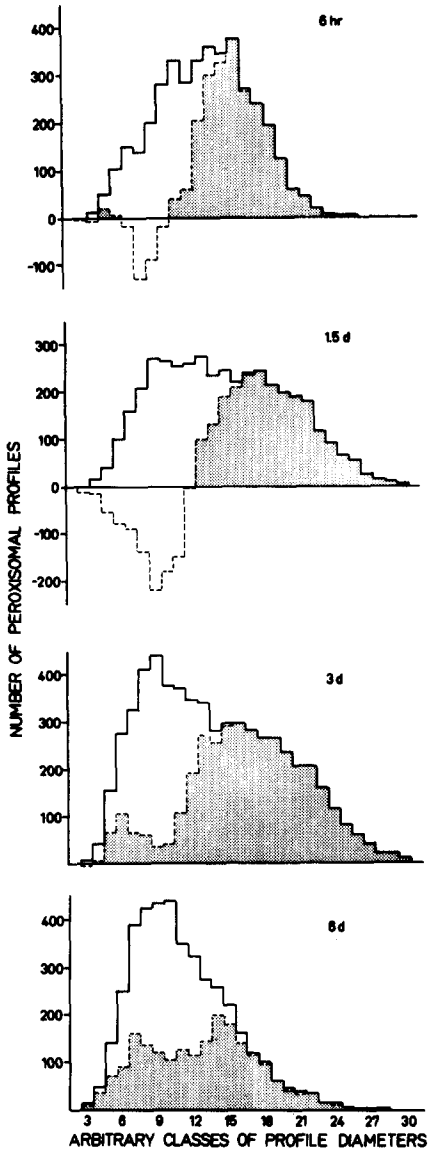

FIGURE 6 A graphic attempt to demonstrate the possibility that a new category of peroxisomes would emerge during drug treatment. For each class of profile diameters, the control value was subtracted from the corresponding value for drug-treated animals (——). The resultant distribution (----) is indicative of the appearance of a drug-induced particle population of a larger size range (shaded areas). The negative values obtained at 6 h and 1.5 days could be interpreted in terms of a relative deficiency of smaller peroxisomes in the size range present in normal hepatocytes. During the recovery period, e.g., on days 3 and 6, the number of larger organelles was gradually reduced (cf. Fig. 5) with a concomitant resurgence of the population of smaller particles. The data refer to equal areas of liver tissue.

TABLE I

Estimation of the Number of "True" Anucleoid Peroxisomes (Microperoxisomes)

Treatment	Number of anucleoid particles in percent of total peroxisomes		
	Based on diameter ratio nucleoid/peroxisome	Based on counts of nucleoid-containing profiles	Difference = "true" anucleoid peroxisomes
Control	57	70	13
Su-13 437 (1.5 days)	73	88	15

proliferative response of PO to the drug is coupled with a relative impoverishment of particles belonging to the control size distribution. This deficit was greatest after 1.5 days, when the mean particle volume had attained its peak value (Fig. 2). Upon withdrawal of Su-13 437, the size range of control particles was progressively refilled.

It is noteworthy that under the stimulation of Su-13 437, the different peroxisomal parameters all reflected the expansion of the PO compartment. However, in comparing the times of occurrence of their respective peak values, some differences were observed. For example, the specific volume of PO was at its maximum on the 3rd day, i.e., 1 day after drug therapy was discontinued (Fig. 1). The highest value of the mean particle volume, however, was reached about 1.5 days earlier (Fig. 2). From this, it might be concluded that the increment in specific volume observed between days 1.5 and 3 (Fig. 1) does not result from a further increase in the particle volume, but may be mainly caused by the reappearance of smaller particles which apparently belong to the size range of the control animals (Fig. 6). In this context, it should be noted that the specific number of PO reached its maximum on day 16 (Fig. 3), most probably through the joint contribution of remaining larger PO and newly recruited smaller ones (Figs. 5 and 6). These relationships are represented in Fig. 7.

BIOSYNTHETIC ASPECTS: Figs. 8 and 9 represent the general aspect of the autoradiographs used for the present analysis at two different magnification and labeling levels. Fig. 8 depicts the situation encountered when the density of developed silver grains were greatest (42 grains/82 μm^2), i.e., 6 h after administration of [^{3}H]arginine. In the course of the experiment, the extent of labeling was reduced as a result of pro-

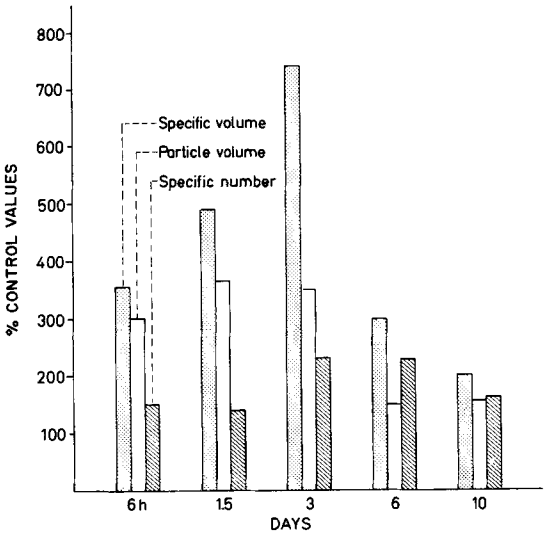

FIGURE 7 Synopsis of the changes displayed by three peroxisomal parameters during drug treatment. It should be noted that their maxima do not coincide in time.

tein turnover. Fig. 9 represents an intermediate stage, i.e., 3 days after the injection of the isotope, when the average grain density amounted to 28 grains/82 μm^2.

Throughout the experiment the ER was the most extensively labeled compartment of the liver parenchymal cell (Table II). In general, the grain density was higher over the RER than over the SER (Table II and Fig. 10); this difference was more pronounced during the early postlabeling stages (Fig. 10). Examination of the specific label density, however, revealed no essential difference in the total grain content between the RER and SER (Fig. 11). It is thus concluded that the silver-grain concentration over the RER and SER was comparable.

As can be seen from Figs. 10 and 11, the time-course of radiation label density (Fig. 10) and specific label density (Fig. 11) of the ER membranes did not follow a more or less exponential curve, as would have been expected if the isotope initially present had been "chased" from the ER by incoming nonradioactive molecules, as a consequence of membrane replacement. Instead, a plateau occurred between days 1.5 and 3. The significance of this observation is not clearly understood, but it should be remembered that the drug treatment was discontinued between these two time-points (cf. Fig. 1). In addition, we have observed that Su-13 437 behaves like a liver-inducing agent.[3] Therefore, in common with some of these agents, such as phenobarbital, it may have the capacity to influence protein metabolism (cf. references 15, 18, 28, 33, 36, and 64). It is thus conceivable that, upon withdrawal of the drug, important metabolic changes might have intervened which could in turn have entailed shifts in metabolic pool sizes. Such alterations might also have markedly influenced the metabolic fate of the reusable isotope. Furthermore, the disposal of PO containing radioactive proteins which occurred during the recovery period may perhaps have contributed a sizable amount of labeled low-molecular products to the metabolic pools.

Although the Golgi apparatus collected a rather limited amount of silver grains (Table II and Fig. 12), its specific label density at 6 h was among the highest observed in all compartments analyzed (Fig. 13).

As previously shown, the dense-body compartment which was defined as including autophagic vacuoles (or cytolysosomes) accounts for a minor volume fraction (0.0106–0.0322 ml/100 g body weight) in the livers of both control and treated animals; in addition, this parameter was not significantly changed as a consequence of drug treatment.[4] Accordingly, the radiation label density exhibited by these organelles was small throughout the duration of the experiment (Table II, Fig. 12). Different results were obtained by plotting the specific label density (Fig. 13). In this case, at the earliest postlabeling time (20 min), the values were in the same range as those of the ER (Fig. 11). At 6 h, however, a peak was observed which was the highest observed in all compartments studied, although it did not significantly differ from the corresponding value for PO. The values then declined sharply until day 3; from then on, the concentration of silver grains over the dense bodies diminished more slowly, possibly because labeled PO, as well as other cytoplasmic components destined for breakdown, had entered this compartment in the form of cytolysosomes.

[3] W. Stäubli, W. Schweizer, and J. Suter, unpublished results. It was found that oral administration of five doses of Su-13 437 (100 mg/kg) to 5-day-old rats caused a (reversible) doubling of the specific surface of hepatocytic SER membranes to ~30 m^2/100 g body weight. Similarly, the specific activity of the microsomal aminopyrine *N*-demethylase was increased from 0.0077 μg formaldehyde formed/mg protein/s (control) to 0.0107 μg/mg protein/s (five doses of Su-13 437).

[4] W. Stäubli and J. Suter, unpublished observations.

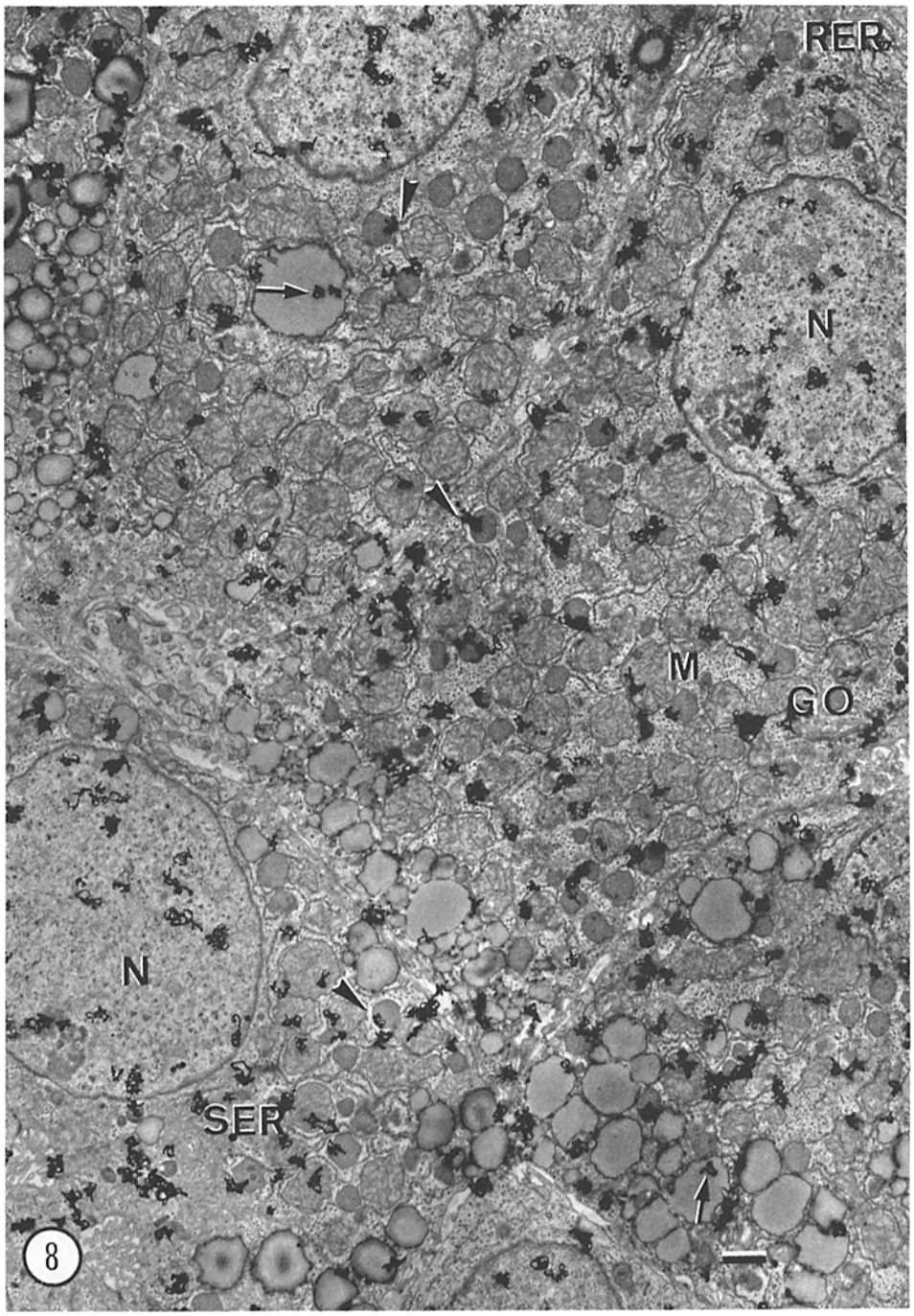

FIGURE 8 Low-power autoradiograph obtained 6 h after administration of [^{3}H]arginine. Note the presence of silver grains over nuclei (*N*), mitochondria (*M*), peroxisomes (arrowheads), rough (*RER*) and smooth (*SER*) endoplasmic reticulum, Golgi region (*GO*), and lipid droplets (arrows). Scale bar, 1 μm. × 6,250.

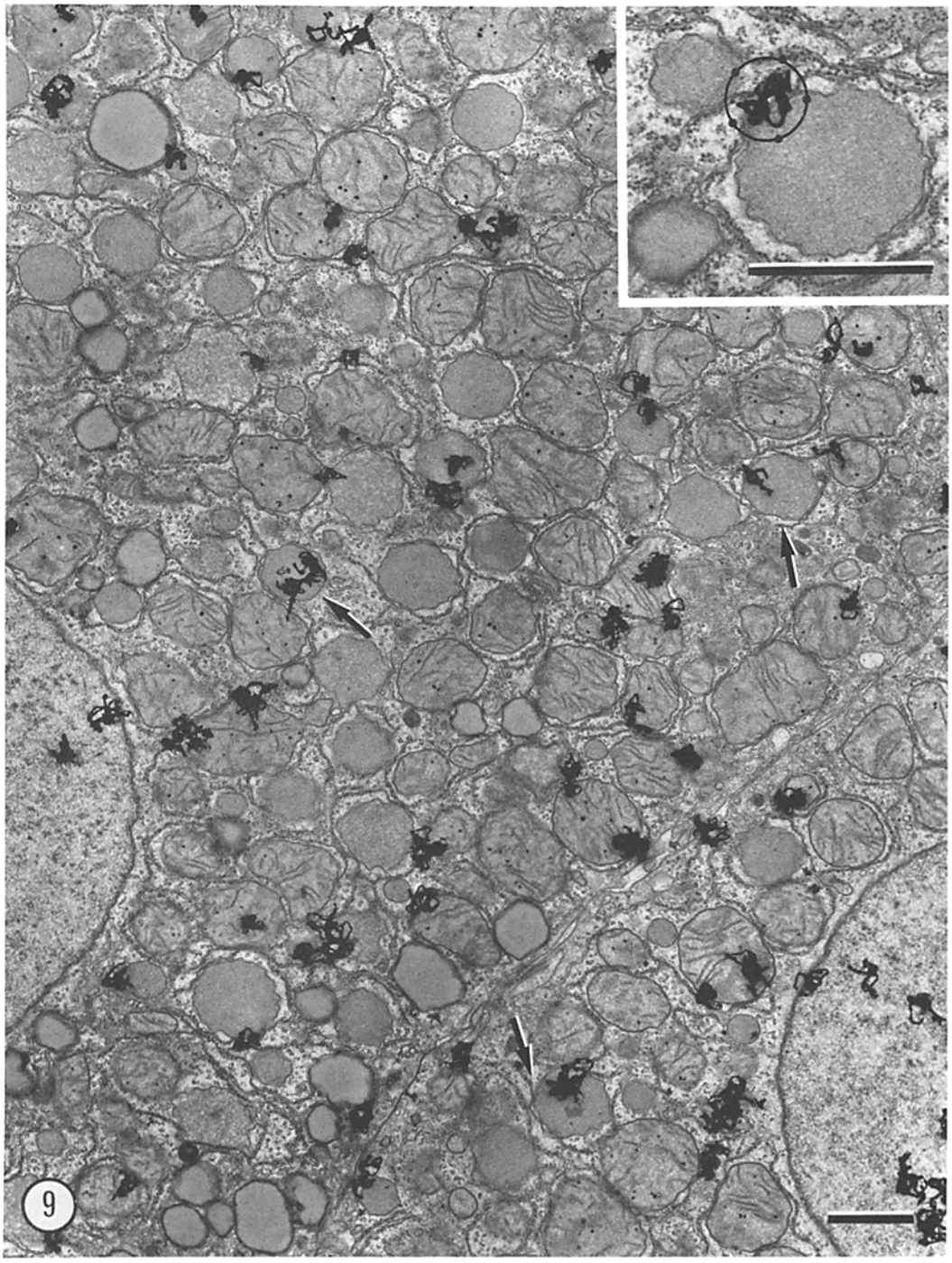

FIGURE 9 Autoradiograph representing parts of two adjacent hepatocytes 3 days after the injection of [^{3}H]arginine. About 10% of the total silver grains could be attributed to the peroxisomes (arrows). Scale bar, 1 μm. × 12,500. *Inset:* Positioning of the resolution-boundary circle (diameter: 12.4 mm) over a developed silver grain. By means of the five equidistant points, the contribution of the different cell compartments to a given silver grain was estimated as exemplified under Materials and Methods. Scale bar, 1 μm. × 27,500.

TABLE II

Distribution of Radiation Label Density in Cell (RV·) between the Main Cellular Compartments of the Hepatocyte

Time after [³H]arginine injection	RER	SER	Mitochondria	Nuclei	Peroxisomes	Golgi	Dense bodies
	%	%	%	%	%	%	%
20 min	39.4	24.5	22.4	7.5	4.2	1.6	0.4
6 h	33.0	23.5	22.7	11.9	6.7	1.8	0.4
1.5 days	33.4	23.2	23.6	7.5	10.1	1.4	0.8
3 days	31.5	20.5	30.0	6.9	10.0	0.7	0.4
6 days	27.3	21.7	30.7	12.9	5.4	1.2	0.8
10 days	31.7	25.9	29.2	7.8	2.4	2.2	0.8

It was interesting to note that the radiation label density of PO was the only parameter studied in the present investigation which displayed a plateau between 6 h and 3 days; after the withdrawal of the drug, the radiation label density of the peroxisomal compartment declined (Table II; Fig. 12). 20 min after administration of the isotope, the specific radiation label density was of the same magnitude (Fig. 13) as that of the ER (cf. Fig. 11). At 6 h, this parameter attained a peak in PO, in contrast to the ER; at 1.5 and 3 days, the specific label density of PO was still higher than at the beginning of the experiment; thereafter, i.e., during the recovery period, the label density per unit volume of PO gradually diminished (Fig. 13).

To establish a relationship between the size of the PO and their label density, we determined the dimensions of labeled and unlabeled peroxisomal profiles by means of the particle size analyzer (Fig. 14). It can be seen that the majority of labeled peroxisomal profiles were found in the larger diameter classes and, thus, followed closely the drug-dependent size increase of the particles. This observation suggests that the isotope, once incorporated into a PO of an expanding population, remained associated with the particle during its enlargement in the course of drug treatment. This finding is more explicitly described in Table III, which indicates the grain distribution over peroxisomal profiles of two different size classes. It is obvious that the ratio of labeled to unlabeled profiles is generally much lower in the small class than

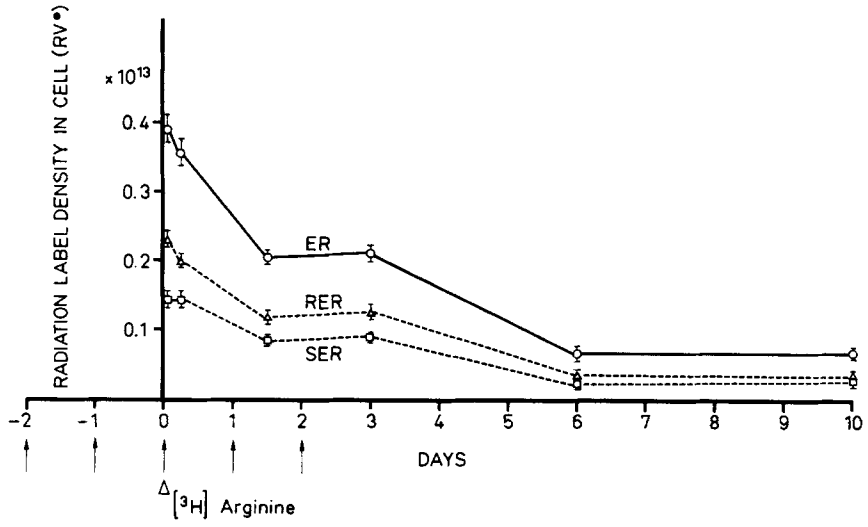

FIGURE 10 Radiation label density of ER membranes in cell (RV·). The labeled amino acid, [³H]arginine, was administered together with the third dose of the drug, i.e., on day 0 (arrowhead). The liver tissue was removed 20 min, 6 h, 1.5, 3, 6, and 10 days after the isotope injection and processed for morphometry and autoradiography. For further experimental details, see Fig. 1. For all parameters, the differences between the following values are not significant: 20 min vs. 6 h, 1.5 vs. 3 days, and 6 vs. 10 days. The differences between all other values are significant. Standard errors are indicated.

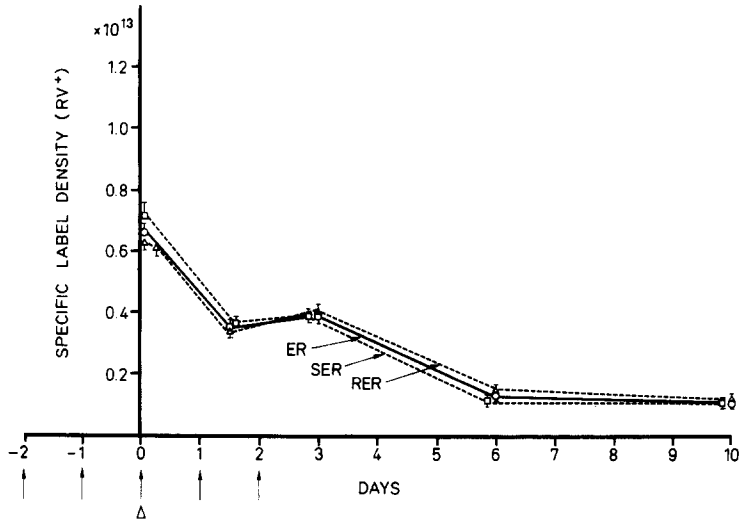

FIGURE 11 Specific label density of ER membranes (RV^+). The following values did not differ significantly: RER, 20 min vs. 6 h, 6 vs. 10 days; SER and ER, 20 min vs. 6 h, 1.5 vs. 3 days, 6 vs. 10 days. All other differences are significant. Standard errors are indicated.

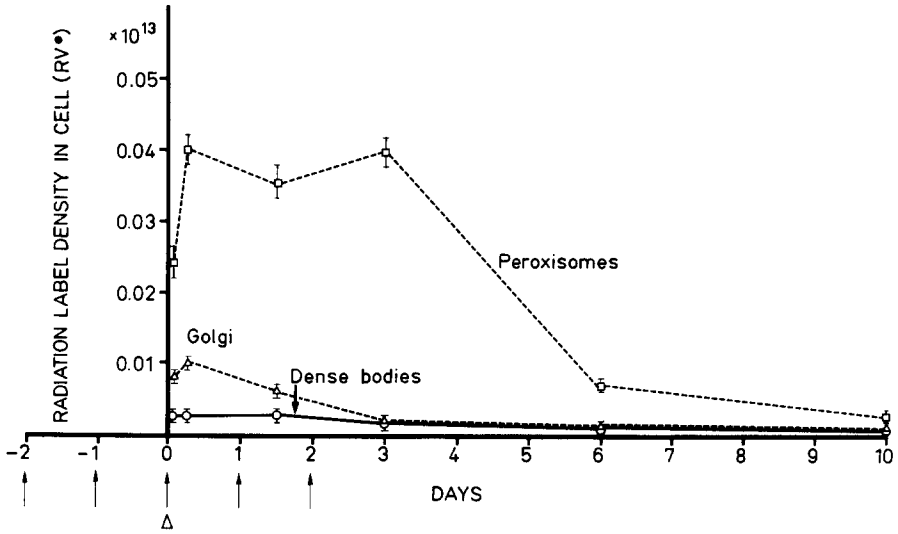

FIGURE 12 Radiation label density of peroxisomes, dense bodies, and Golgi apparatus in cell ($RV^\cdot$). The differences between the following means are not significant: peroxisomes, 6 h vs. 1.5 days, 6 h vs. 3 days, 1.5 vs. 3 days; dense bodies, 20 min vs. 6 h, 20 min vs. 1.5 days, 20 min vs. 3 days, 20 min vs. 6 days, 6 h vs. 1.5 days, 6 h vs. 3 days, 6 h vs. 6 days, 1.5 vs. 3 days, 3 vs. 6 days, 3 vs. 10 days, 6 vs. 10 days; Golgi, 20 min vs. 6 h, 20 min vs. 1.5 days, 20 min vs. 10 days, 1.5 vs. 3 days, 1.5 vs. 10 days, 3 vs. 10 days, 6 vs. 10 days. All other differences are significant. Standard errors are indicated.

in the large class, suggesting a preferential incorporation of the isotope into the larger-sized organelles. With the continuation of treatment, i.e., between 6 h and 3 days, the ratio of labeled to unlabeled small profiles progressively diminished. In contrast, the extent of labeling of the larger particles remained constant, and only declined when the drug was withdrawn. Closer inspection of Fig. 14 reveals that the smallest labeled peroxisomal profiles were somewhat larger than the smallest unlabeled profiles. As the experiment proceeded, the size of the smallest labeled particle

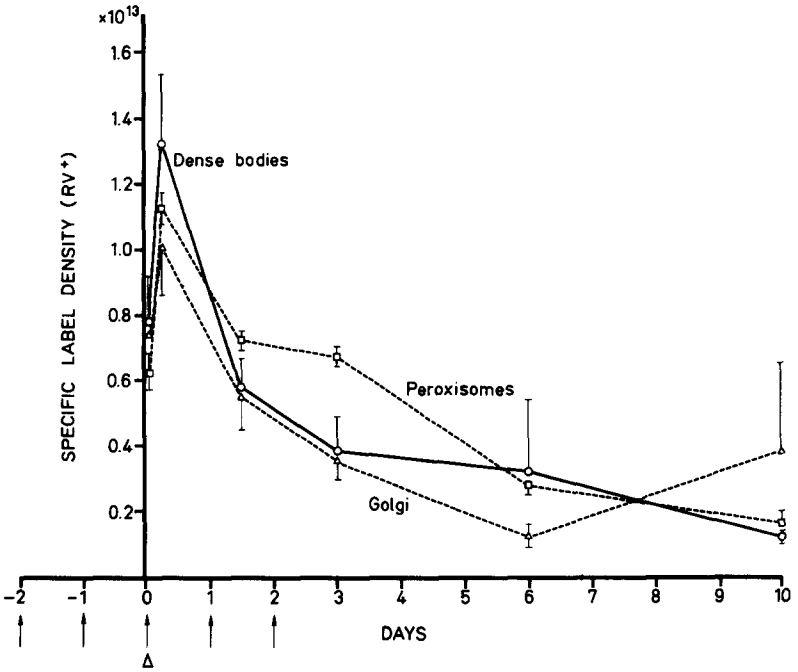

FIGURE 13 Specific label density of peroxisomes, dense bodies, and Golgi apparatus (RV^+). The differences between the following means are not significant: peroxisomes, 20 min vs. 1.5 days, 20 min vs. 3 days, 1.5 vs. 3 days, 6 vs. 10 days; dense bodies, 20 min vs. 6 h, 20 min vs. 1.5 days, 20 min vs. 6 days, 1.5 vs. 3 days, 1.5 vs. 6 days, 3 vs. 6 days, 6 vs. 10 days; Golgi, 20 min vs. 6 h, 20 min vs. 1.5 days, 20 min vs. 10 days, 1.5 vs. 3 days, 1.5 vs. 10 days, 3 vs. 10 days, 6 vs. 10 days. All other differences are significant. Standard errors are indicated.

profile gradually shifted to higher diameter classes (cf. arrowheads on the abscissa of Fig. 14), indicating that the isotope distribution reflected the drug-induced size changes occurring within the peroxisomal population.

Biochemical Findings

In untreated animals, the activity of some of the peroxisomal enzymes tended to increase moderately toward the end of the experiment (Tables IV and V), in accordance with the postnatal activity pattern established for rat liver (74).

It was anticipated from the uniform staining behavior of the expanding peroxisomal population after peroxidase cytochemistry (results not shown) that the biochemically determined catalase activity of hepatic mitochondrial fractions isolated from drug-treated animals would be enhanced. In fact, as shown in Table IV, the specific activity of this enzyme in the MLP fractions obtained from rats that had received five doses of Su-13 437 was lower than that of the corresponding control fractions. In contrast, the soluble fraction of livers of treated animals displayed a considerable catalase activity, which reached a peak at the stage of greatest expansion of the peroxisomal compartment (Fig. 1). During recovery from medication, this enzyme activity tended to return to control levels (Table IV). The most obvious explanation for this drug-related shift in the subcellular distribution of catalase activity is that this enzyme was in part leached-out from the PO of treated animals. This interpretation was supported to some extent by observations made on Millipore-filtered MLP fractions (Fig. 15). If such fractions were treated according to the DAB procedure in order to reveal peroxidase activity, most of the reactive particles showed an inhomogeneous distribution of the reaction product within their matrix. The appearance of variable proportions of the matrical space completely devoid of histochemical stain suggested that a loss of DAB-reactive material from most of cell-free PO had probably occurred during preparation of the cell fractions. Apparently, part of the leached-out peroxisomal catalase appeared in the soluble fraction; however, the sum of enzyme activities recovered in the MLP and soluble fractions of treated animals did not

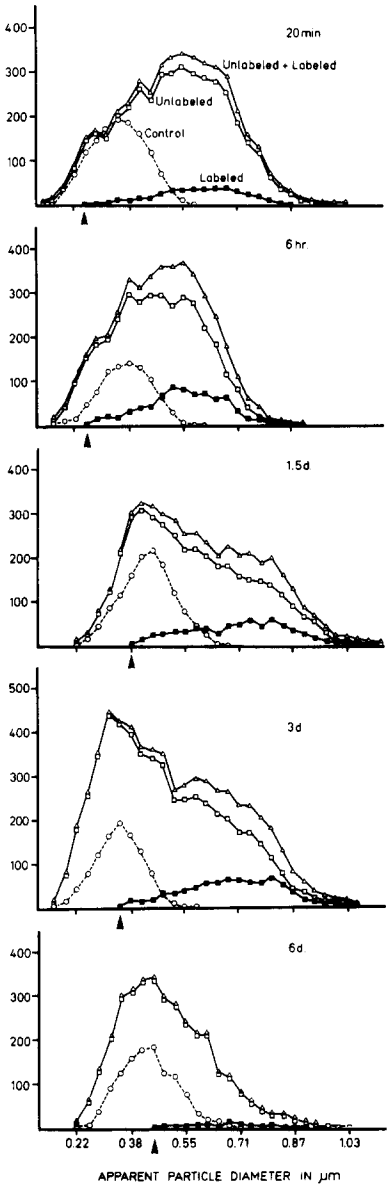

FIGURE 14 Distribution of silver grains over peroxisomal profiles of various size classes after the administration of [^{3}H]arginine. A profile was registered as labeled if more than half of the area covered by a grain was located within the perimeter of the profile. The arrowheads point to the smallest labeled profiles. For comparison, the size distribution of control peroxisomes is shown.

much exceed those of the control fractions (Table IV), as would have been expected from roughly a sixfold increase of peroxisomal specific volume (Fig. 1). There are several possible explanations to account for this obvious discrepancy. (*a*) It has been shown in liver homogenate of CPIB- or nafenopin-treated rats that the increase in the activity or content of catalase was regularly less prominent than the proliferative response of the peroxisomal compartment (26, 57, 61). (*b*) In treated animals, a relatively greater proportion of catalase might cosediment with microsomal structures (76) which were not analyzed in the present study. (*c*) Part of the "solubilized" peroxisomal catalase could have been adsorbed on microsomal membranes.

Treatment of infant rats with five doses of Su-13 437 moderately depressed the specific activity of the core enzyme urate oxidase (Table V).

Recovery Period

Upon cessation of drug treatment, all the PO-related parameters declined, thus demonstrating the reversibility of the proliferation process. This applied to the specific volume (Fig. 1) and the mean volume (Fig. 2) as well as to the specific number (Fig. 3). The contraction of the peroxisomal compartment during the recovery period proceeded gradually. As can be seen in Figs. 5 and 6, the number of drug-induced larger particles was continuously reduced. Concomitantly, the PO of smaller size classes, which were numerically reduced during drug treatment, were gradually refilled (Fig. 6). As a result of these two processes, the overall size distributions of PO finally reapproached the control shape (Fig. 5).

It follows from the foregoing considerations that the disposal of the excess PO formed in the presence of Su-13 437 is an important aspect of the recovery period. In general agreement with observations of Svoboda and Reddy (72), our evidence indicates that two different destruction mechanisms might be operative in the hepatocytes. The first process is considered to be of an autophagic nature, whereas the second can be described as consisting of a "dissolution" of individual PO within the cytoplasmic matrix, apparently without the involvement of segregating membranes (cf. reference 70).

The liver-inducing capacity of nafenopin has already been documented (cf. footnote 3). It could be argued that the disposal of the excess of SER membranes and PO during the regression phase would necessarily have called for an activation of the lysosomal system. As demonstrated earlier, neither the volume density nor the numerical density of these organelles was remarkably increased during the recovery period (cf. footnote

TABLE III

*Ratio of Labeled to Unlabeled "Small" and "Large" Peroxisomal Profiles**

Time after [³H]arginine injection	Number of labeled peroxisomal profiles		Number of unlabeled peroxisomal profiles		Ratio of labeled to unlabeled profiles	
	Small	Large	Small	Large	Small	Large
20 min	29	365	1,012	3,082	1:35	1:8.4
6 h	77	654	1,220	2,384	1:16	1:3.7
1.5 days	41	596	1,337	2,539	1:33	1:4.3
3 days	24	727	2,117	3,245	1:88	1:4.5
6 days	4	67	1,693	1,755	1:423	1:26.2

* The limit between "small" and "large" peroxisomal profiles was arbitrarily set at a diameter of 0.3833 μm. The small diameter class would comprise the bulk of particles whose diameters fall within the size distribution of control peroxisomes (cf. Fig. 5).

TABLE IV

Subcellular Distribution of Hepatic Catalase Activity

Subcellular fraction	Experimental time-point	Catalase activity		
		Control	Treated	P*
		μmol/mg protein/s		
Mitochondria (MLP fraction)	6 h	29.07±5.76‡	13.59±2.08	<0.001
	1.5 days	18.51±4.14	10.36±3.48	>0.05
	3 days	26.75±6.88	18.61±2.74	>0.05
	6 days	22.24±2.28	32.73±3.91	<0.001
	10 days	42.57±3.63	49.29±4.16	<0.05
Postmicrosomal supernate (S fraction)	6 h	0.99±0.64 (6/6)§	7.76±0.57 (6/6)	<0.001
	1.5 days	0.29 (1/5)	9.76±0.22 (5/5)	–
	3 days	0.21 (2/6)	10.80±0.50 (6/6)	<0.001
	6 days	0.27 (4/6)	6.36±0.84 (6/6)	<0.001
	10 days	0.02 (1/6)	0.64 (4/6)	–
Fraction MLP + S	6 h	30.06	21.26	
	1.5 days	18.80	20.12	
	3 days	26.96	29.41	
	6 days	22.51	39.09	
	10 days	42.75	49.93	

* Level of significance.

‡ Standard deviation.

§ Numerical ratio of animals showing a detectable enzyme activity to total number of animals.

TABLE V

Urate Oxidase Activity of the Mitochondrial Fraction (MLP Fraction)

Experimental time-point	Urate oxidase activity		
	Control	Treated	P*
	nmol/mg protein/h		
6 h	228.2±50.0‡	165.1±113.4	>0.05
1.5 days	325.9±135.5	284.9±125.7	>0.05
3 days	521.4±228.6	300.4±71.9	<0.05
6 days	262.9±99.9	201.5±130.4	>0.05
10 days	348.5±108.4	240.1±50.5	>0.05

* Level of significance.

‡ Standard deviation.

4). Similarly, the specific label density of dense bodies displayed no important changes during the restitution phase (Fig. 13), indicating that this compartment did not receive a sizable portion of radioactive material from those structures, i.e., SER and PO, which, by virtue of their drug-induced proliferation, would have suffered a particularly extensive breakdown.

DISCUSSION

General Considerations

In evaluating the results presented in this paper,

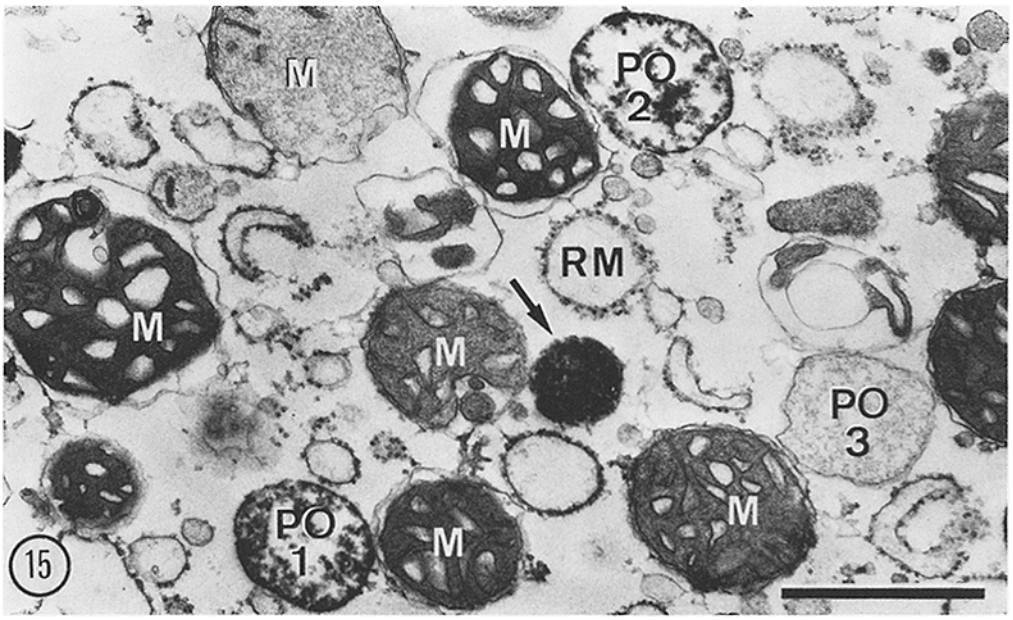

FIGURE 15 The DAB procedure for peroxidase as applied to Millipore pellicles obtained from MLP fractions reveals that the great majority of peroxisomes contain only residual patches of electron-dense deposits (particles labeled *PO 1* and *PO 2*) or possibly no reaction product at all (structure labeled *PO 3*, which admittedly could also represent a damaged mitochondrion). The arrow indicates one of the rare peroxisomal profiles completely filled with reaction product and thus resembling the organelles usually encountered in DAB-reacted tissue sections. Scale bar, 1 μm. × 27,000.

it is important to bear in mind the particular conditions under which the experiments were carried out. Because liver tissue of postnatal rats was used, it was to be expected that during the experimental period (7th to 17th day postpartum) the metabolism of liver parenchymal cells would be subject to a series of complex developmental alterations (21, 34, 43), thus precluding the establishment of steady-state conditions in the tissue as a whole. Nevertheless, however marked the diversity in the developmental kinetics of some important morphological and biochemical parameters of the maturing hepatocyte may be, the specific volume and number of mitochondria (results not presented) and of peroxisomes (Figs. 1 and 3) tended to be stable throughout the period of observation.

It seems reasonable to assume that the administration of the hypolipidemic drug Su-13 437 (nafenopin) to newborn rats might profoundly influence the metabolic dynamics of the hepatocyte differentiation process. In this respect, it should be mentioned that this drug, in addition to being an excellent peroxisome-proliferating agent, also caused liver induction and an elevation of the specific volume and number of mitochondria (data not shown).

Autoradiographic Observations

If the time-course of the radiation label density (Fig. 10) and the specific label density (Fig. 11) of the different ER membranes is followed, it can be seen that these parameters were highest 20 min after the injection of the isotope, and declined from then on. In contrast to the labeling pattern displayed by the ER membranes, the grain concentration over the Golgi complex was lower 20 min after the administration of the isotope than after 6 h (Figs. 12 and 13), indicating that at least part of the labeled material had shifted from the ER to the Golgi membranes during this time interval. This distribution of labeled material is entirely compatible with the well-established observation that many proteins synthesized by the hepatocyte for extracellular destinations display an ordered migration within sequentially arranged cytoplasmic membrane systems (17, 32, 48, 53).

It was interesting to note that the dense bodies exhibited the highest specific label density of all

compartments analyzed (Fig. 13). The accumulation of silver grains over these particles is apparently not due to a drug-induced increase in lysosomal activity, because in hepatocytes of untreated animals the lysosomes also showed a high grain concentration (1), in accordance with recent biochemical findings indicating a high turnover rate of lysosomal proteins (75).

The majority of the autoradiographic parameters had reached a minimum 6 days after the injection of [^{3}H]arginine, except in the Golgi apparatus. Between the 6th and 10th postlabeling day, the specific label density of this membrane system was considerably increased (Fig. 13). In unpublished experiments, we have observed that the number of Golgi-associated secretion vacuoles containing lipoprotein particles was reversibly reduced during drug treatment. It is thus conceivable that the increase in the silver-grain concentration over Golgi elements on day 10 (Fig. 13) reflects the restoration of their activity. It should be mentioned that the very low density lipoproteins of human and rabbit serum contain an arginine-rich apoprotein species (67, 68) which may preferentially carry the label found over Golgi-associated structures in the autoradiographs.

Proliferative Response of Peroxisomes

It is well established that the treatment of adult rodents with the lipid-lowering agents CPIB (clofibrate), Su-13 437 (nafenopin), or SaH-42 348 results in a proliferative response of PO (20, 30, 39, 42, 47, 56, 70). Recent evidence points to the possibility that this expansion of the peroxisomal compartment is causally linked to the hypolipidemic action of these agents (39, 58). The present study demonstrates that the drug Su-13 437 also leads to an activation of the peroxisomal compartment of neonatal rats, manifested in a large (approximately sixfold) increase in the specific volume (Fig. 1) and a moderate (approximately twofold) rise in the specific number (Fig. 3). The expanding state of PO was also reflected by the autoradiographic data. For example, the radiation label density, as expressed in percent of total grain counts, increased in a roughly dose-dependent manner up to the 3rd day, whereas in the other compartments the same parameter remained stable or declined. On the 3rd postlabeling day, the PO occupied ~6% of the hepatocytic cytoplasm and had assembled ~10% of the total silver grains (Table II). These findings suggest that the proliferating PO incorporated a considerable amount of the isotope, in accordance with biochemical observations which indicate a high incorporation activity of expanding PO (42).

As a consequence of the discrepancy between the numerical increase and the volumetric increase of expanding PO mentioned above, a part of them responded to the presence of the drug with a gradual enlargement (Figs. 2, 5, and 6), resulting in a relatively broad and flat size distribution of the whole particle population, which extended from ~0.2 to ~1.0 μm in diameter (Fig. 5). It is noteworthy that the expanding particle population still included, though in a smaller relative number, PO of the size range encountered in control animals (Fig. 5). This observation suggests that the whole expanding PO population may be composed of at least two subpopulations. One of these is thought to consist of particles showing the control pattern of size distribution and the tendency to diminish in number during drug treatment. The other subpopulation would be constituted by PO responding to the drug stimulus with proliferation and enlargement. However, we did not succeed, by graphical means, in demonstrating unambiguously that the overall drug-induced size pattern of treated rats was the result of two overlapping distributions made up of "control" and "drug-induced" particles, respectively. This failure was probably related to the fact that either our treatment schedule did not establish steady-state conditions under which a maximal separation of the subpopulation would possibly have occurred, or the particle counts were suboptimal. Nevertheless, when the particle population of control livers was subtracted from the experimental distribution, it became obvious that the latter was somewhat deficient in smaller PO (Fig. 6), in spite of an increase in the total number of PO (Fig. 3).

In fact, a large body of evidence lends support to our hypothesis that the PO formed under medication with aryloxyisobutyric acid derivatives display a particular behavior, and thus represent a class of peroxisomes unique in various respects. (*a*) There is an increased frequency of anucleoid PO profiles (Fig. 4) which apparently is not related to an augmentation of the so-called microperoxisomes (Table I), but instead reflects an altered balance between nucleoids and matrical constituents in the enlarged PO (Figs. 2 and 5). (*b*) The subcellular distribution of hepatic catalase activity

indicated that part of this enzyme must have been lost from the peroxisome-rich mitochondrial fraction and displaced to the postmitochondrial supernate (Table IV). This finding is in accordance with recently published work in which the various aspects of the distributional effects of Su-13 437 (42) and SaH-42 348 (47) on peroxisomal enzymes have been comprehensively discussed. A similar compartmental redistribution of catalase activity was also encountered in the livers of CPIB-treated rats and interpreted in terms of a preferential leaching-out of catalase from PO (25, 26, 35, 42, 47), eventually leading to particles which, in a cell-free state, contain a reduced catalase complement (Fig. 15). In fact, it has been reported that this enzyme is a most readily solubilized component of PO (22, 46) and may be used as a marker of the physical integrity of these organelles (22). In addition, we have observed that hepatic PO isolated from livers of CPIB-treated rats tended to reach a lower density than those from untreated animals during centrifugation in Ficoll density gradients (25); in a recent study, it was shown that CPIB treatment caused the emergence of a less dense rat liver PO class (23). Furthermore, it has been pointed out that during drug-induced expansion of PO, the numerical increase in peroxisomal particles largely exceeded the increase (approximately twofold) in liver catalase activity or concentration, suggesting the occurrence of relatively catalase-deficient PO (57, 61). This interpretation is supported by observations indicating that during treatment with CPIB (40) of Su-13 437 (42) a part of hepatic PO stained less intensively with the DAB procedure than did PO of untreated animals. (*c*) A considerably altered enzyme pattern is exhibited by aryloxyisobutyric acid-induced PO (3, 20, 26, 39, 42, 47, 71). (*d*) The labeling behavior of PO during their proliferative phase did not fit a Poisson distribution (Table VI), indicating that only a certain part of the whole particle population had incorporated the isotope. In contrast, the grain distribution over mitochondria, in accordance with other findings (9), tended to satisfy the requirements of a Poisson distribution (Table VI), as would have been expected for the labeling of a metabolically homogeneous population. (*e*) Drug-induced PO were observed to display distinctive morphologic characteristics, such as a more pronounced variation in size and shape (20, 41, 42, 57, 59, 73), eccentrically located nucleoids (51), an altered electron density of the matrix (41, 42), or the occurrence of special matrical structures (29, 57).

Biosynthesis of Peroxisomes

Shortly after the injection of a radioactive amino acid (20 min), the specific label density of PO was found to be in the region of that recorded for the ER membranes (Figs. 11 and 13). This finding might suggest that both compartments are equally well supplied with the isotope; but it does not, of course, prove the widely accepted notion that the PO represent locally differentiated zones of the ER (cf. references 7, 29, 47, 60). As the grain concentration over the ER was declining, presumably as a result of a migrational efflux of proteins, the specific label density of PO reached its peak 6 h after isotope administration (Fig. 13). Thus, between 20 min and 6 h the PO received additional amounts of radioactive material, most probably at the expense of the ER radioactivity. These observations suggest a different temporal labeling behavior of the ER and PO, compatible with the timing of catalase biosynthesis (38). For several obvious reasons, autoradiographic analysis

TABLE VI

Chi-Square Test of Silver Grain Distribution over Mitochondrial and Peroxisomal Profiles during Volumetric Expansion of the Peroxisomal Compartment

Time after [^{3}H]arginine injection	Grain number	Mitochondria: Grain number per profile 0	1	2	3	4	χ^2	Peroxisomes: Grain number per profile 0	1	2	3	χ^2
6 h	Observed	9,080	1,853	169	17	1	3.5	3,565	642	33	0	11.8
	Theoretical	9,086.6	1,834.5	185.2	12.5	0.67		3,588.3	598.9	50.0	2.8	
1.5 days	Observed	9,919	1,363	74	3	0	3.6	4,034	598	22	1	10.2
	Theoretical	9,937.4	1,329.6	88.9	3.9	0.1		4,052.1	561.2	38.9	1.8	
3 days	Observed	11,538	1,832	110	12	0	10.6	5,713	831	30	1	14.3
	Theoretical	11,558.0	1,788.3	138.3	7.1	0.3		5,739.6	780.0	53.0	2.4	

For 1° of freedom $\chi^2_{0.05} = 3.84$; for 2° of freedom, $\chi^2_{0.005} = 5.99$.

is not suited to substantiate and extend biochemical findings on the biosynthetic pathway of specific peroxisomal constituents at the subcellular level, i.e., to disclose the structural features of the cytosolic catalase intermediate(s) (38).

Growth of Peroxisomes

Assuming our hypothesis that the drug-induced expansion of the peroxisomal compartment is mainly the result of the *de novo* formation and subsequent growth of a special class of particles is correct, the problem of peroxisomal growth has to be considered briefly. The available biochemical evidence suggests that the initially proposed "budding and growth" model (13) may no longer be regarded as a plausible interpretation of the biosynthetic pathway of PO in the liver cells of untreated rats (12). Instead, it has been proposed that PO are not individualized organelles with a fixed life-span, but may continuously interchange material by means of interconnecting (ER) channels (12, 60), or by fusional and/or fissional processes occurring at the level of the peroxisomal particles (40, 59). Accordingly, the whole PO population of a hepatocyte might be considered to represent a single metabolic pool, in which peroxisomal material could flow unrestrictedly. The most plausible interpretation of the results presented here does not concur with such an assumption. It was observed that after the administration of the isotope, the specific label density of PO remained elevated as long as the drug was administered and then declined rapidly (Fig. 13). This conserved radioactivity was associated preferentially with the larger PO, the smaller ones being less extensively labeled (Table III and Fig. 14). As the drug-induced expansion of PO progressed further, the frequency peak of labeled particles moved to larger size classes (Fig. 14), which displayed a high level of labeling (Table III). Similarly, the limit of the smallest labeled particles was displaced to larger diameter classes (Fig. 14). These findings suggest that the proliferation of a class of larger PO is the outcome of a unique metabolic process initiated and maintained by agents endowed with a PO-stimulating capacity. The gradual and progressive nature of this drug-induced shift in size and radioactivity is difficult to reconcile with the hypothesis that the whole PO population of the hepatocyte constitutes a homogeneous metabolic compartment. On the other hand, these observations are compatible with the expansion of a particular class of particles by growth.

In the context of this label shift to PO of a larger diameter, a methodological aspect of autoradiography should be considered. It has been shown that, through the spread of radiation, smaller radioactive sources occurring in autoradiographs might be at a disadvantage in comparison with larger ones (66). However, the data given by Salpeter and McHenry (66) indicate that, in view of the small average dimensional changes associated with the peroxisome expansion, this size-dependent preferential labeling of larger particles could only have influenced our determinations slightly.

Disposal of Peroxisomes during the Recovery Period

At least three pathways have been proposed for the disposal of the excess of PO formed during treatment with aryloxyisobutyric derivatives (42, 47, 72). The first process is considered to be autophagic by nature, whereas the second one is described as consisting of a "dissolution" or "atrophy" of individual PO within the cytoplasmic matrix, without the involvement of sequestering membranes. A third breakdown mechanism has been tentatively described as proceeding by means of a retraction of PO contents within the SER compartment (47); it is conceivable that the two last-mentioned processes are morphologically interconnected. Using cytochemical procedures, we have studied, during the reconstitution period, the disappearance of the excess of PO formed in the presence of Su-13 437 (70). The results obtained could be interpreted in terms of the first two pathways mentioned. In addition, we have presented evidence suggesting the possibility that the "dissolution" of PO (42, 72) might be assisted by acid-phosphatase-positive elongated cisternae; these structures were seen to be appressed to or intercalated between PO displaying a matrix of reduced electron density (70). Although we have not quantitatively assessed the parts played by the different structures tentatively involved in the destruction of PO, silver grains lying over both sequestered and "dissolving" PO were rarely observed. Apparently, the intracellular removal of the excess PO proceeded gradually (Figs. 5 and 6); in keeping with this observation, the specific number and volume of dense bodies, including autophagic vacuoles, were not dramatically

changed during the recovery period (cf. footnote 4). This observation is at variance with the findings reported by Moody and Reddy (47). These authors noted a significant increase of the lysosomal volume density in adult rat hepatocytes 4 days after withdrawal of SaH-42 348. Nevertheless, it seems possible that in the neonatal situation the recovering hepatocyte is capable of removing, within a few days, a large number of organelles without being compelled to build up an extensive destruction apparatus. Similar observations were made in rat liver cells after the discontinuation of CPIB treatment (72), or during glucagon-induced autophagy (16). The process leading to the destruction of PO must obviously entail a certain capacity to select PO of a larger size out of a PO population which, during the recovery period, comprises an increasing amount of smaller particles (Figs. 5 and 6). Thus, in the case of Su-13 437-treated neonatal rats, the breakdown of the drug-induced excess of PO seems not to be a strictly random process such as has been suggested to occur in normal adult liver to explain the exponential decay kinetics of labeled peroxisomal proteins (12, see also reference 54).

The authors are grateful to Dr. H. Bittiger for his valuable comments. We acknowledge the help of Dr. H. Eckert and Mr. U. Spornitz in preparing autoradiographs. We also wish to thank Mrs. Christiane Zimmerman, Miss Gabrielle Jobin, and Mr. Max Schlienger for excellent technical assistance. The help of Dr. H. R. Gnägi in the computation of data and Mrs. Josette Chollet, Mrs. Anne-Marie Kyburz, Mr. A. H. Kirkwood, M. A., Miss Gertrud Reber, and Mr. Karl Babl in preparing the manuscript is gratefully acknowledged.

Received for publication 5 December 1975, and in revised form 27 January 1977.

REFERENCES

1. ASHLEY, C. A., and T. PETERS, Jr. 1969. Electron microscopic radioautographic detection of sites of protein synthesis and migration in liver. *J. Cell Biol.* **43:**237–249.
2. AZARNOFF, D. L. 1971. Pharmacology of hypolipidemic drugs. *Fed. Proc.* **30:**827–828.
3. AZARNOFF, D. L., and D. SVOBODA. 1966. Changes in microbodies in the rat induced by ethyl *p*-chlorophenoxyisobutyrate. *J. Lab. Clin. Med.* **68:**854.
4. BAUDHUIN, P. 1968. L'analyse morphologique quantitative de fractions subcellulaires. Thèse. Université catholique de Louvain.
5. BAUDHUIN, P., H. BEAUFAY, Y. RAHMAN-LI, O. Z. SELLINGER, R. WATTIAUX, P. JACQUES, and C. de DUVE. 1964. Tissue fractionation studies-17. Intracellular distribution of monoamine oxidase, aspartate aminotransferase, alanine aminotransferase, D-amino acid oxidase and catalase in rat liver tissue. *Biochem. J.* **92:**179–184.
6. BAUDHUIN, P., P. EVRARD, and J. BERTHET. 1967. Electron microscopic examination of subcellular fractions. I. The preparation of representative samples from suspensions of particles. *J. Cell Biol.* **32:**181–191.
7. BEARD, M. E., and A. B. NOVIKOFF. 1969. Distribution of peroxisomes (microbodies) in the nephron of the rat: a cytochemical study. *J. Cell Biol.* **42:**501–508.
8. BERGERON, M., and B. DROZ. 1968. Analyse critique des conditions de fixation et de préparation de tissus pour la détection radioautographique des protéines néoformées, en microscopie électronique. *J. Microsc.* **7:**51–62.
9. BERGERON, M., and B. DROZ. 1969. Protein renewal in mitochondria as revealed by electron microscope radioautography. *J. Ultrastruct. Res.* **26:**17–30.
10. CARO, L. G. 1961. Electron microscopic radioautography of thin sections: the Golgi zone as a site of protein concentration in pancreatic acinar cells. *J. Biophys. Biochem. Cytol.* **10:**37–45.
11. CREASEY, W. A. 1960. The enzymic composition of nuclei from radio-sensitive and non-sensitive tissues with special reference to catalase activity. *Biochem. J.* **77:**5–12.
12. DE DUVE, C. 1973. Biochemical studies on the occurrence, biogenesis and life history of mammalian peroxisomes. *J. Histochem. Cytochem.* **21:**941–948.
13. DE DUVE, C., and P. BAUDHUIN. 1966. Peroxisomes (microbodies and related particles). *Physiol. Rev.* **46:**323–357.
14. DE DUVE, C., B. C. PRESSMAN, R. GIANETTO, R. WATTIAUX, and F. APPELMANS. 1955. Tissue fractionation studies. 6. Intracellular distribution patterns of enzymes in rat liver tissue. *Biochem. J.* **60:**604–617.
15. DEHLINGER, P. J., and R. T. SCHIMKE. 1972. Effect of phenobarbital, 3-methylcholanthrene, and hematin on the synthesis of protein components of rat liver microsomal membranes. *J. Biol. Chem.* **247:**1257–1264.
16. DETER, R. L. 1971. Quantitative characterization of dense body, autophagic vacuole, and acid phosphatase-bearing particle populations during the early phases of glucagon-induced autophagy in rat liver. *J. Cell Biol.* **48:**473–489.
17. GLAUMANN, H., and J. L. E. ERICSSON. 1970. Evidence for the participation of the Golgi apparatus in the intracellular transport of nascent albumin in the liver cell. *J. Cell Biol.* **47:**555–567.

18. GLAZER, R. I., and A. C. SARTORELLI. 1972. The effect of phenobarbital on the synthesis of nascent protein on free and membrane-bound polyribosomes of normal and regenerating liver. *Mol. Pharmacol.* **8:**701–710.
19. GNÄGI, H. R., P. H. BURRI, and E. R. WEIBEL. 1970. A multipurpose computer program for automatic analysis of stereological data obtained on electron micrographs. 7ème Congrès International de Microscopie Electronique. Grenoble. **1:**443–444.
20. GOLDENBERG, H., M. HÜTTINGER, P. KAMPFER, R. KRAMAR, and M. PAVELKA. 1976. Effect of clofibrate application on morphology and enzyme content of liver peroxisomes. *Histochemistry.* **46:**189–196.
21. GREENGARD, O. 1969. The hormonal regulation of enzymes in prenatal and postnatal rat liver: effects of adenosine 3′,5′-(cyclic)-monophosphate. *Biochem. J.* **115:**19–24.
22. HAYASHI, H., T. SUGA, and S. NIINOBE. 1973. Studies on peroxisomes. III. Further studies on the intraparticulate localization of peroxisomal components in the liver of the rat. *Biochim. Biophys. Acta.* **297:**110–119.
23. HAYASHI, H., T. SUGA, and S. NIINOBE. 1975. Studies on peroxisomes. V. Effect of ethyl *p*-chlorophenoxyisobutyrate on the centrifugal behavior of rat liver peroxisomes. *J. Biochem.* **77:**1199–1204.
24. HESS, R., R. MAIER, and W. STÄUBLI. 1969. Evaluation of phenolic ethers as hypolipidaemic agents: effects of CIBA 13, 437-Su. *Adv. Exp. Med. Biol.* **4:**483–489.
25. HESS, R., W. RIESS, and W. STÄUBLI. 1967. Hepatic actions of hypolipidemic drugs: effect of ethyl chlorophenoxyisobutyrate (CPIB). *Prog. Biochem. Pharmacol.* **2:**325–336.
26. HESS, R., W. STÄUBLI, and W. RIESS. 1965. Nature of the hepatomegalic effect produced by ethylchlorophenoxyisobutyrate in the rat. *Nature (Lond.).* **208:**856–858.
27. HIGASHI, T., and T. PETERS, JR. 1963. Studies on rat liver catalase. II. Incorporation of ^{14}C-leucine into catalase of liver cell fractions in vivo. *J. Biol. Chem.* **238:**3952–3954.
28. HOLTZMAN, J. L. 1969. Effect of chronic phenobarbital administration on the turnover of hepatic microsomal protein. *Biochem. Pharmacol.* **18:**2573–2576.
29. HRUBAN, Z., M. GOTOH, A. SLESERS, and S.-F. CHOU. 1974. Structure of hepatic microbodies in rats treated with acetylsalicylic acid, clofibrate, and dimethrin. *Lab. Invest.* **30:**64–75.
30. HRUBAN, Z., and M. RECHCIGL, JR. 1969. Microbodies and related particles: morphology, biochemistry and physiology. *Int. Rev. Cytol. Suppl.* **1.**
31. HRUBAN, Z., E. L. VIGIL, A. SLESERS, and E. HOPKINS. 1972. Microbodies: constituent organelles of animal cells. *Lab. Invest.* **27:**184–191.
32. JAMIESON, J. C., and F. E. ASHTON. 1973. Studies on acute phase proteins of rat serum. IV. Pathway of secretion of albumin and α_1-acid glycoprotein from liver. *Can. J. Biochem.* **51:**1281–1291.
33. KATO, R., L. LOEB, and H. V. GELBOIN. 1965. Microsome-specific stimulation by phenobarbital of amino acid incorporation in vivo. *Biochem. Pharmacol.* **14:**1164–1166.
34. KNOX, W. E. 1972. Enzyme Patterns in Fetal, Adult and Neoplastic Rat Tissues. S. Karger, Basel. 198.
35. KRISHNAKANTHA, T. P., and C. K. R. KURUP. 1972. Increase in hepatic catalase and glycerol phosphate dehydrogenase activities on administration of clofibrate and clofenapate to the rat. *Biochem. J.* **130:**167–175.
36. KURIYAMA, Y., T. OMURA, P. SIEKEVITZ, and G. E. PALADE. 1969. Effects of phenobarbital on the synthesis and degradation of the protein components of rat liver microsomal membranes. *J. Biol. Chem.* **244:**2017–2026.
37. LAZAROW, P. B., and C. DE DUVE. 1973. The synthesis and turnover of rat liver peroxisomes. IV. Biochemical pathway of catalase synthesis. *J. Cell Biol.* **59:**491–506.
38. LAZAROW, P. B., and C. DE DUVE. 1973. The synthesis and turnover of rat liver peroxisomes. V. Intracellular pathway of catalase synthesis. *J. Cell Biol.* **59:**507–524.
39. LAZAROW, P. B., and C. DE DUVE. 1976. A fatty acyl-CoA oxidizing system in rat liver peroxisomes: enhancement by clofibrate, a hypolipidemic drug. *Proc. Natl. Acad. Sci. U. S. A.* **73:**2043–2046.
40. LEGG, P. G., and R. L. WOOD. 1970. Effects of catalase inhibitors on the ultrastructure and peroxidase activity of proliferating microbodies. *Histochemie.* **22:**262–276.
41. LEGG, P. G., and R. L. WOOD. 1970. New observations on microbodies: a cytochemical study on CPIB-treated rat liver. *J. Cell Biol.* **45:**118–129.
42. LEIGHTON, F., L. COLOMA, and C. KOENIG. 1975. Structure, composition, physical properties, and turnover of proliferated peroxisomes: a study of the trophic effects of Su-13 437 on rat liver. *J. Cell Biol.* **67:**281–309.
43. LEVINE, S., and R. F. MULLINS, JR. 1966. Hormonal influences on brain organization in infant rats. *Science (Wash. D.C.).* **152:**1585–1592.
44. LOUD, A. V. 1968. A quantitative stereological description of the ultrastructure of normal rat liver parenchymal cells. *J. Cell Biol.* **37:**27–46.
45. LOWRY, O. H., N. J. ROSEBROUGH, N. J. FARR, and R. J. RANDALL. 1951. Protein measurement with the Folin phenol reagent. *J. Biol. Chem.* **193:**265–275.
46. MARKWELL, M. A. K., E. J. MCGROARTY, L. L. BIEBER, and N. E. TOLBERT. 1973. The subcellular distribution of carnitine acyl-transferases in mam-

malian liver and kidney: a new peroxisomal enzyme. *J. Biol. Chem.* **248:**3426-3432.
47. MOODY, D. E., and J. K. REDDY. 1976. Morphometric analysis of the ultrastructural changes in rat liver induced by the peroxisome proliferator SaH 42-348. *J. Cell Biol.* **71:**768-780.
48. MORGAN, E. H., and T. PETERS, JR. 1971. Intracellular aspects of transferrin synthesis and secretion in the rat. *J. Biol. Chem.* **246:**3508-3511.
49. NOVIKOFF, A. B., and P. M. NOVIKOFF. 1973. Microperoxisomes. *J. Histochem. Cytochem.* **21:**963-966.
50. NOVIKOFF, P. M., A. B. NOVIKOFF, N. QUINTANA, and C. DAVIS. 1973. Studies on microperoxisomes. III. Observations on human and rat hepatocytes. *J. Histochem. Cytochem.* **21:**540-558.
51. NOVIKOFF, P. M., P. S. ROHEIM, A. B. NOVIKOFF, and D. EDELSTEIN. 1974. Production and prevention of fatty liver in rats fed clofibrate and orotic acid diets containing sucrose. *Lab. Invest.* **30:**732-750.
52. PETERS, T., JR., and C. A. ASHLEY. 1969. Binding of amino acids to tissues by fixatives. *In* Autoradiography of Diffusible Substances. L. J. Roth and W. E. Stumpf, editors. Academic Press Inc., New York. 267-278.
53. PETERS, T., JR., B. FLEISCHER, and S. FLEISCHER. 1971. The biosynthesis of rat serum albumin. IV. Apparent passage of albumin through the Golgi apparatus during secretion. *J. Biol. Chem.* **246:**240-244.
54. POOLE, B. 1971. The kinetics of disappearance of labeled leucine from the free leucine pool of rat liver and its effect on the apparent turnover of catalase and other hepatic protein. *J. Biol. Chem.* **246:**6587-6591.
55. POOLE, B., F. LEIGHTON, and C. DE DUVE. 1969. The synthesis and turnover of rat liver peroxisomes. II. Turnover of peroxisome proteins. *J. Cell Biol.* **41:**536-546.
56. REDDY, J. 1973. Possible properties of microbodies (peroxisomes): microbody proliferation and hypolipidemic drugs. *J. Histochem. Cytochem.* **21:**967-971.
57. REDDY, J., D. L. AZARNOFF, D. SVOBODA, and J. D. PRASAD. 1974. Nafenopin-induced hepatic microbody (peroxisome) proliferation and catalase synthesis in rats and mice. *J. Cell Biol.* **61:**344-358.
58. REDDY, J., and T. P. KRISHNAKANTHA. 1975. Hepatic peroxisome proliferation: induction by two novel compounds structurally unrelated to clofibrate. *Science (Wash. D.C.).* **190:**787-789.
59. REDDY, J., and D. SVOBODA. 1971. Microbodies in experimentally altered cells. VIII. Continuities between microbodies and their possible biologic significance. *Lab. Invest.* **24:**74-81.
60. REDDY, J., and D. SVOBODA. 1973. Further evidence to suggest that microbodies do not exist as individual entities. *Am. J. Pathol.* **70:**421-438.
61. REDDY, J., D. SVOBODA, and D. L. AZARNOFF. 1973. Microbody proliferation in liver induced by nafenopin, a new hypolipidemic drug: comparison with CPIB. *Biochem. Biophys. Res. Commun.* **52:**537-543.
62. REDMAN, C. M., D. J. GRAB, and R. IRUKULA. 1972. The intracellular pathway of newly formed rat liver catalase. *Arch. Biochem. Biophys.* **152:**496-501.
63. REYNOLDS, E. S. 1963. The use of lead citrate at high pH as an electron-opaque stain in electron microscopy. *J. Cell Biol.* **17:**208-213.
64. RUDDON, R. W., and C. H. RAINEY. 1970. Stimulation of nuclear protein synthesis in rat liver after phenobarbital administration. *Biochem. Biophys. Res. Commun.* **40:**152-160.
65. SALPETER, M. M., and L. BACHMANN. 1965. Assessment of technical steps in electron microscope autoradiography. *In* The Use of Radioautography in Investigating Protein Synthesis. C. P. Leblond and K. B. Warren, editors. Academic Press Inc., New York. 23-39.
66. SALPETER, M. M., and F. A. MCHENRY. 1973. Electron microscope autoradiography: analyses of autoradiograms. *In* Advanced Techniques in Biological Electron Microscopy. J. K. Koehler, editor. Springer-Verlag, Berlin, and New York. 113-152.
67. SHORE, B., V. SHORE, A. SALEL, D. MASON, and R. ZELIS. 1974. An apolipoprotein preferentially enriched in cholesteryl ester-rich very low density lipoproteins. *Biochem. Biophys. Res. Commun.* **58:**1-7.
68. SHORE, V., and B. SHORE. 1973. Heterogeneity of human plasma very low density lipoproteins: separation of species differing in protein components. *Biochemistry.* **12:**502-507.
69. STÄUBLI, W., and R. HESS. 1966. Quantitative aspects of hepatomegaly induced by ethylchlorophenoxy-isobutyrate (CPIB). *In* Proceedings of the 6th International Congress on Electron Microscopy. R. Ueda, editor. Maruzen Co., Ltd., Tokyo. **2:**625-626.
70. STÄUBLI, W., and R. HESS. 1975. Lipoprotein formation in the liver cell: ultrastructural and functional aspects relevant to hypolipidemic action. *Handb. Exp. Pharmacol.* **41:**229-289.
71. SVOBODA, D., H. GRADY, and D. L. AZARNOFF. 1967. Microbodies in experimentally altered cells. *J. Cell Biol.* **35:**127-152.
72. SVOBODA, D., and J. REDDY. 1972. Microbodies in experimentally altered cells. IX. The fate of microbodies. *Am. J. Pathol.* **67:**541-554.
73. TSUKADA, H., Y. MOCHIZUKI, M. ITABASHI, M. GOTOH, and H. P. MORRIS. 1975. Response of microbodies in Morris hepatoma 9618A to clofibrate. *J. Natl. Cancer Inst.* **55:**153-158.
74. TSUKADA, H., Y. MOCHIZUKI, and T. KONISHI. 1968. Morphogenesis and development of microbodies of hepatocytes of rats during pre- and postna-

tal growth. *J. Cell Biol.* **37**:231–243.
75. WANG, C.-C., and O. TOUSTER. 1975. Turnover studies on proteins of rat liver lysosomes. *J. Biol. Chem.* **250**:4896–4902.
76. WATTIAUX, R., and S. WATTIAUX-DE CONINCK. 1968. Particules subcellulaires dans les tumeurs. I. Distribution intracellulaire de la cytochrome oxydase, la glucose-6-phosphatase, la catalase et plusieurs hydrolases acides dans un hépatome chimique transplantable (hépatome HW). *Eur. J. Cancer.* **4**:193–200.
77. WEDEL, F. P., and E. R. BERGER. 1975. On the quantitative stereomorphology of microbodies in rat hepatocytes. *J. Ultrastruct. Res.* **51**:153–165.
78. WEIBEL, E. R., W. STÄUBLI, H. R. GNÄGI, and F. A. HESS. 1969. Correlated morphometric and biochemical studies on the liver cell. I. Morphometric model, stereologic methods, and normal morphometric data for rat liver. *J. Cell Biol.* **42**:68–91.
79. WHUR, P., A. HERSCOVICS, and C. P. LEBLOND. 1969. Radioautographic visualization of the incorporation of galactose-^{3}H and mannose-^{3}H by rat thyroids in vitro in relation to the stages of thyroglobulin synthesis. *J. Cell Biol.* **43**:289–311.
80. WICKSELL, S. D. 1925. On the size distribution of sections of a mixture of spheres. *Biometrika.* **17**:84–99.